UNIVERSITY OF NAPLES FEDERICO II

PH.D. PROGRAM IN

CLINICAL AND EXPERIMENTAL MEDICINE

CURRICULUM IN TRANSLATIONAL PEDIATRIC SCIENCES

XXXII Cycle

(Years 2017-2020)

Chairman: Prof. Francesco Beguinot

PH.D. THESIS

TITLE

SECONDARY ABNORMALITIES IN LYSOSOMAL STORAGE DISEASES

TUTOR

Prof. Giancarlo Parenti

PH.D. STUDENT

Dr. Carla Damiano

INDEX

General introduction

Pompe disease

Pompe disease (PD) is a metabolic myopathy caused by mutations of the GAA gene, resulting in functional deficiency of the lysosomal hydrolase acid α-glucosidase (GAA, acid maltase, E.C.3.2.1.20). [Van der PLoeg et al, 2008] Deficiency of acid α-glucosidase leads to accumulation of lysosomal glycogen in virtually all cells of the body, but the effects are most notable in muscles. [Hirschhorn et al,2001] The estimated incidence of PD has been reported to vary between 1:40,000 and 1:146,000. [Van der Ploeg et al, 2008; Semplicini et al, 2018] Newborn screening programs implemented in some countries are changing this figure, with incidence rates of approximately 1: 17,000-1:27,000. [Scott et al, 2013; Bodamer et al, 2017; Chien et al, 2019]

The GAA gene, localized in 17q25.2-q25.3, consists of 20 exons spread over 28 kb of genomic sequence and encodes for a protein of 952 amino acids with a predicted molecular mass of 110 kDa. [Hoefsloot et al, 1990] The 110 kDa GAA protein synthesized in the endoplasmic reticulum is a precursor polypeptide, which undergoes N-glycan processing in the Golgi apparatus, and is proteolytically processed in the lysosomes into active isoforms of 76 and 70 kDa, through an intermediate molecular form of 95 kDa. [Hoefsloot et al, 1990]

The mature enzyme hydrolyzes the alpha-1,4 and 1,6-glycosidic bonds of glycogen, releasing glucose units that are then transported across the lysosomal membrane by a specific carrier.

Being GAA deficiency ubiquitous in PD, glycogen storage occurs in almost every tissue and cell type. However, disease manifestations are predominantly related to muscle involvement and heart and skeletal muscle are the major sites of pathology.

So far more than 500 different GAA gene variations have been identified (The Human Gene Mutation Database, HGMD and Pompe Center) and the type of mutation correlates in most cases with the residual enzyme activity. GAA activity may range from complete deficiency (<1%) in the severe forms, to partial (up to 30%) deficiency in milder forms. PD is often due to missense mutations in GAA gene that causes the synthesis of a misfolded enzyme protein.

Traditionally, PD patients have been classified into distinct categories, including an early onset “classical” form, early onset intermediate phenotypes, and the attenuated late onset juvenile and adult forms.

The “classic” infantile-onset form represents the severe end of this spectrum with a clearly defined phenotype, characterized by severe hypertrophic cardiomyopathy typical ECG pattern, generalized hypotonia and a rapidly progressive course. When untreated, classic infantile PD patients die by the end of the first year. [Van den Hout et al, 2003; Kishnani et al, 2006]

In the late-onset, slowly progressive juvenile and adult-onset forms symptoms related to skeletal muscle dysfunction, resulting in both mobility and respiratory problems, are the primary manifestations. [Hagemans et al, 2005] The first symptoms usually start between the second and fourth decade and are in most instances related to impaired mobility and limb-girdle weakness. The age at onset, the rate of disease progression and the sequence of respiratory and skeletal muscle involvement vary substantially among different patients. The clinical variability makes diagnosis difficult and, in several cases, the final diagnosis is made many years after the start of symptoms. Intermediate phenotypes (early onset without cardiomyopathy, childhood-onset) have also been described and characterized.

Therapy for PD: Enzyme replacement therapy

The only approved treatment for PD is enzyme replacement therapy (ERT) with recombinant human GAA (rhGAA). ERT is based on the concept that recombinant lysosomal hydrolases, in most cases enzyme precursors manufactured on large scale in eukaryotic cells systems (chinese hamster ovary cells), can be administered periodically to patients by an intravenous route. RhGAA binds to the mannose 6-phosphate receptor, which is present on the cell surface of cardiomyocytes and skeletal muscle cells. The enzyme is then internalized into the myocyte and transported via endocytosis to the lysosome. Inside the lysosome, rhGAA breaks down the accumulated glycogen into glucose. [Reuser et al, 1984; Van der Ploeg et al,1991] Major beneficial effects of enzyme therapy in infants are very encouraging, but leave no doubt that the treatment of patients with classic infantile Pompe's disease is very challenging because of the combination of profound deficiency of acid α-glucosidase, the difficulty of targeting muscle, and the time needed to remodel the muscle fibres and restore the muscle function. The results obtained in infants hold promise for patients with residual acid α-glucosidase activity and a less progressive clinical course. [Van der Ploeg et al, 2008]

However, limitations of ERT are becoming evident. First, not all patients respond equally well to treatment. Second, it is now clear that skeletal muscle (one of the major sites of disease and an important target of therapy) is more refractory to treatment than other tissues. Why this happens remains to be fully elucidated. It has been proposed that several factors concur in reducing the effectiveness of ERT in skeletal muscle. One of these factors is the preferential uptake of rhGAA by liver and the insufficient targeting of the enzyme to skeletal muscle. [Raben et al,2003] The large mass of skeletal muscle and the relative deficiency of the mannose-6-phosphate receptors in muscle cells [Wenk et al,1991] also contribute to the poor correction of GAA activity.

The pathophysiology of PD

Recently, it became clear that a number of pathogenic mechanisms, such as autophagy, calcium homeostasis, oxidative-stress, and mitochondrial abnormalities, all contribute to tissue damage in PD as well as in other LSDs. [Kohler et al, 2018] Autophagy is a dynamic process involving the rearrangement of subcellular membranes to sequester cytoplasm and organelles in autophagic vesicles for delivery to lysosomes or vacuoles where the sequestered cargo is degraded and recycled. [Klionsky et al, 2007] For autophagy to accomplish its biological function (i.e. the turn-over of macromolecules and organelles), autophagic vesicles must fuse to lysosomes to form autophagolysosomes. When autophagy is blocked protein turn-over is impaired, causing the accumulation of ubiquitinated protein aggregates. The presence of large pools of autophagic debris in skeletal muscle and the impact of this pathology on therapy warrant the classification of PD into a group of disorders known as autophagic myopathies. [Nishino et al, 2003] Furthermore, it has been shown that the autophagic build-up affects the trafficking and delivery of the recombinant enzyme to the lysosome. Thus, in PD, a profoundly disordered intracellular recycling system appears to be an important contributor to muscle weakness and incomplete response to treatment. [Kohler et al, 2018]

Aim of the thesis

The general aims of the project of my thesis are to investigate the mechanisms involved in the pathophysiology and to identify novel biomarkers for the treatment of PD that may translate into improved efficacy of the existing therapies. Although the biochemistry and genetics of PD are well known already for many years the pathophysiology is still incompletely clear. Glycogen storage in cells and tissues and impairment of autophagy have been well characterized, however other secondary abnormalities of cellular pathways need further characterization. The first aim of the project is to better characterize the secondary dysregulation of cellular pathways triggered by storage in PD, and to investigate whether these abnormalities may represent novel therapeutic targets, complementary to existing therapies. The second aim of this research project is focused the potential of microRNAs (miRNAs) as new tool for understanding of the disease pathophysiology and as new potential biomarkers to follow disease diagnosis, progression and follow up of patients.

Chapter 1

EVIDENCE OF INCREASED OXIDATIVE-STRESS IN PD. A NEW THERAPEUTIC TARGET?

Introduction

Autophagy and oxidative-stress: cross-talk and redox signalling

Increased oxidative-stress is one of the potential factors implicated in induction of autophagy. Oxidative-stress is defined as a “state in which oxidation exceeds the antioxidant systems in the body, secondary to a loss of the balance between them.” Oxidative-stress plays an important role in the pathophysiology of many diseases. The reactive oxygen species (ROS) in biological systems including superoxide anion (2O2), hydroxyl radical (HO), nitric oxide (NO), peroxyl radical (ROO) and non-radical hydrogen peroxide (H2O2) compose the most important components of oxidative-stress. [Babior, 2000]

ROS and RNS likely act as the intracellular “alarm molecules” of the availability of nutrients, signal their presence and activate the autophagic machinery. ROS-sensitive transcription factors and oxidative response give the cellular warning according to the redox condition [Chuang et al, 2002]. These signal proteins are two signal pathways belonging to two different families. The first of these pathways is mitogen-activated protein (MAP) kinase family and in this pathway phosphorylation occurs starting in from cytoplasm and continuing to nucleus by the activities of extracellular signal regulator kinases, which are c-jun N terminal kinase and p38 MAP kinase. The second family is redox-sensitive signal pathway; cytoplasmic signal factors includes thioredoxin reductase, thioredoxin, nuclear factor Ref-1 and a few transcription factors (AP-1, nuclear factor kappa B (NF-kB), Nfr-1 and Egr-1). Autophagy is required for removing the conditions that cause ox-stress (starvation), for clearing ROS and RNS from cells, and ultimately for allowing cells to overcome conditions of starvation and oxidative-stress [Filomeni et al, 2015].

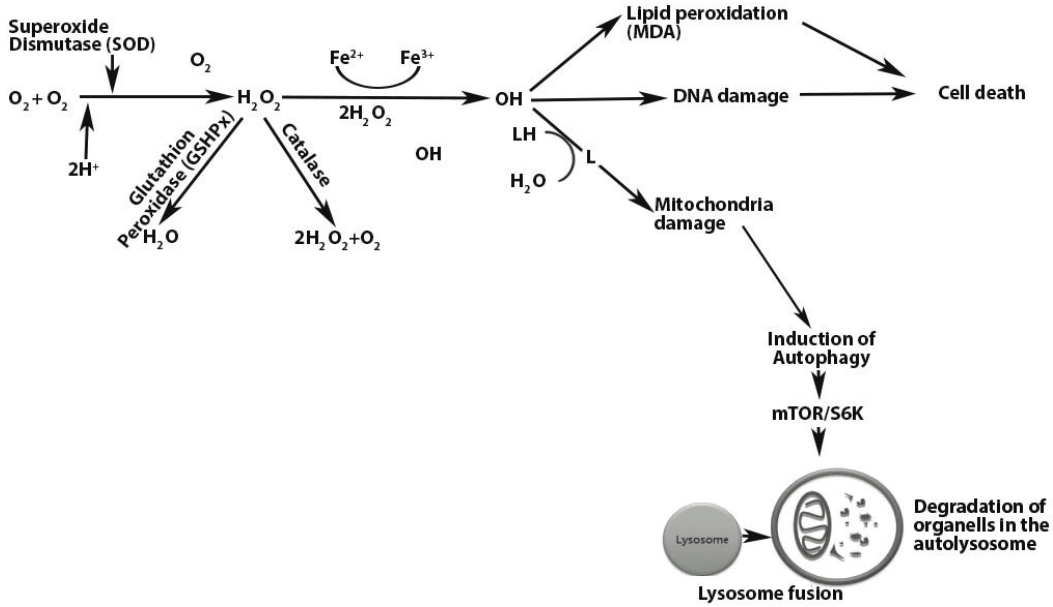

Fig1.**Oxidative-stress mediated cell damages in the cell:** Excessive ROS production can lead to damages in mitochondria, which can cause cell death or oxidative-damaged cell components are degraded by autophagy and promote cell survival

Autophagy is a catabolic pathway activated in response to different cellular stressors, such as damaged organelles, accumulation of misfolded or unfolded proteins, ER stress, accumulation of reactive oxygen species, and DNA damage that is critical to maintain cellular homeostasis. There are three major recognized types of autophagy: microautophagy, chaperone-mediated autophagy (CMA) and macroautophagy,

Microautophagy is a constitutive and sometimes selective process by which whole portions of the cytoplasm are engulfed by direct invagination of lysosomal membrane into tubulovesicular structures. [Ravikumar et al,2010]

CMA is characterized by the translocation of cytosolic proteins into lysosomal lumen. In this process, protein import is directly mediated by the lysosomal-associated membrane protein type 2A (LAMP2A) translocation complex. [Cuervo et al, 2010]

Macroautophagy is the best characterized form of autophagy. It is responsible for the breakdown of proteins and organelles in the cell, and it is considered necessary for cell survival. [Navarro-Yepes et al, 2014] During this process, a portion of cytoplasm including soluble materials and organelles is sequestered within a phagophore, a de novo-formed double-membraned structure also named isolation membrane. After elongation, the phagophore closes upon itself to form a discrete double-membrane autophagic vesicle, called autophagosome, which entraps sequestered cytosolic cargoes. Subsequently, via cytoskeleton-dependent motion, autophagosome engages and fuses with lysosome in a Ca2+-dependent manner, forming a fusion-hybrid organelle called autolysosome. Within the autolysosome, lysosomal enzymes degrade cargoes and the resulting macromolecules are transported back to cytosol for recycling. [Yang et al,2009] When autophagic process is completed, lysosomes are reformed from the fusion-hybrid organelles through lysosome biogenesis.

mTOR (mammalian target of rapamycin), which is a factor playing important role in autophagic activation, is a kinase signal pathway. This signal pathway is classically activated in case of hunger, hypoxia or stress condition. [Levine et al,2005] mTOR complexes exist in two types, namely mTORC1 and mTORC2, which are distinguished by different components. The active mTORC1 prevents autophagy by phospho-inhibiting the UNC51-like kinase 1 (ULK1) at Ser757 that interacts with two partners: the autophagy related gene 13 (Atg13) and the FAK-family interacting protein of 200 kDa (FIP200). These three proteins form together the so called ULK1 complex. [Yang et al, 2010; Nazio et al, 2013] When cells suffer hypoxia, energy depletion, and other

stimuli, mTORC1 activity is simultaneously restrained with the activation of autophagy. When mTORC1 is inhibited, ULK1 is activated and is able to phosphorylate Atg13 and FIP200. This is the first step that leads to the autophagosome formation.

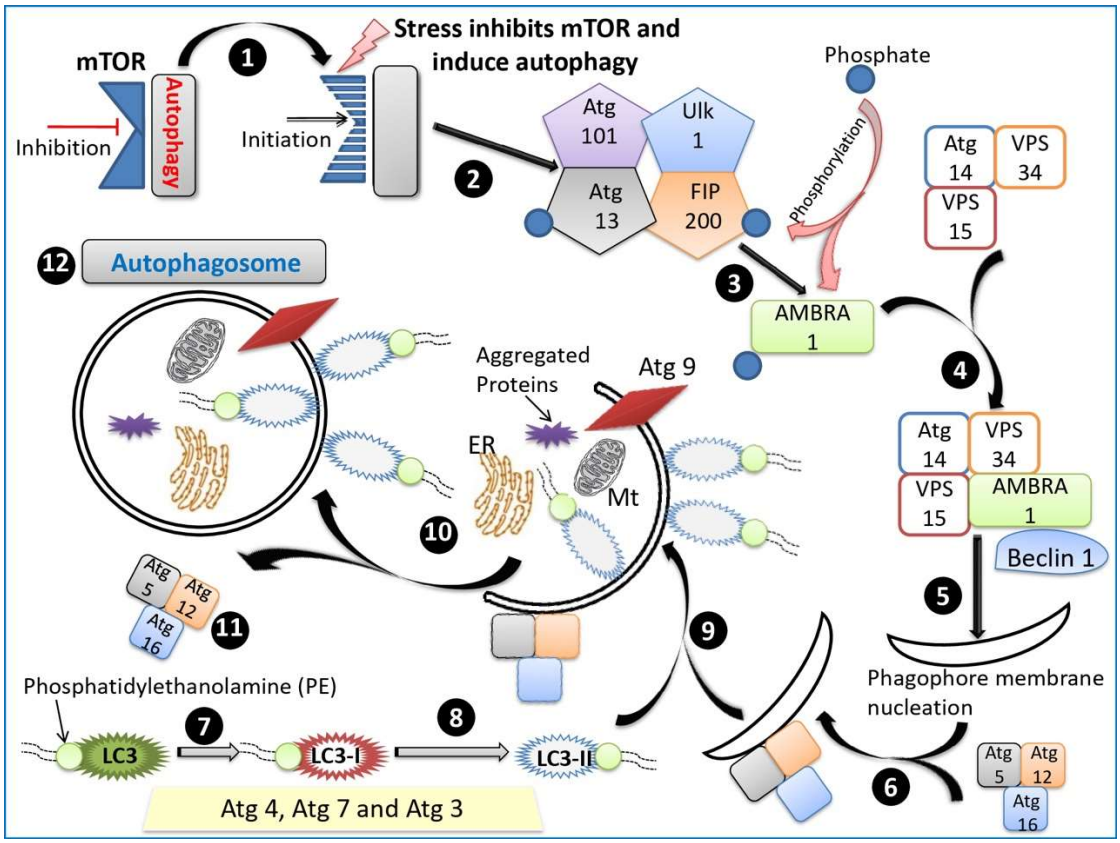

Fig2.**Process of autophagosome formation.** Autophagy is inhibited by mTOR. Various kinds of stress (hypoxia, oxidative-stress, pathogen infection, endoplasmic reticulum stress or nutrient starvation conditions) inhibit mTOR, and the process of autophagy is initiated.

mTOR, represents the main kinase responsible for Transcription factor EB (TFEB) phosphorylation in presence of amino acids. TFEB has arisen as a master regulator of lysosome function and autophagy. In the presence of nutrients TFEB is phosphorylated by mTOR on S142 and S211 serine residues, which play a crucial role in determining TFEB subcellular localization. [Settembre et al,2102] Once in the nucleus, TFEB drives the expression of several genes controlling lysosomal functions, through the

CLEAR (Coordinated Lysosomal Enhancement And Regulation) signaling network. [Medina et al 2015; Sardiello et al, 2009] Furthermore, following an elevation in ROS production or an increase in exogenous oxidants, Mucolipin TRP channel 1-mediated Ca2+ release promoted calcineurin-dependent TFEB nuclear translocation, thus enhancing autophagy and lysosome biogenesis and mitigating oxidative stress. [Zhang et al, 2016]

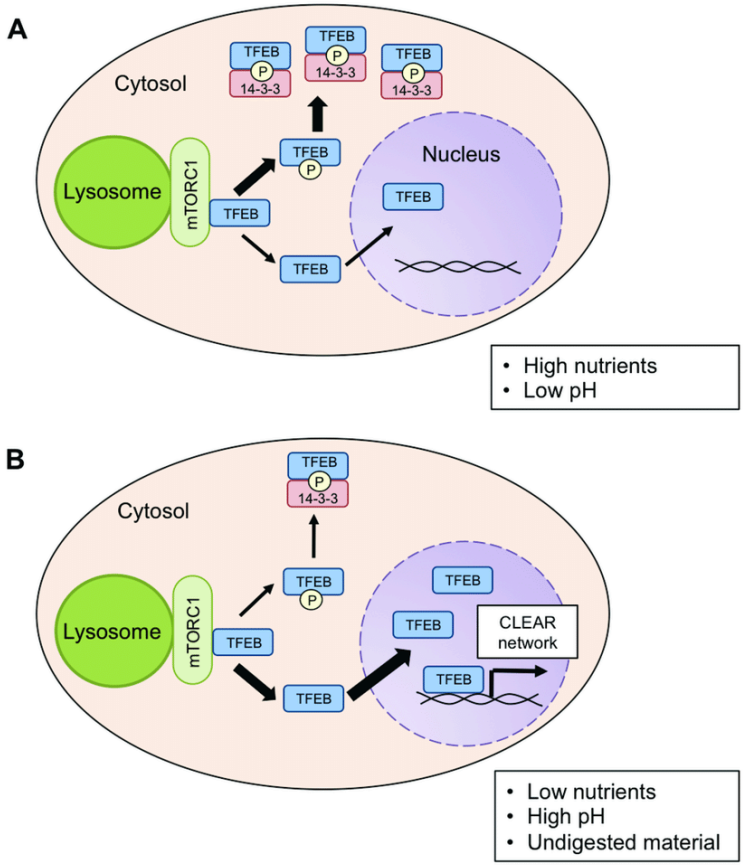

Fig3.**Mechanisms of TFEB activation** A. TFEB is inactivated under optimal lysosomal conditions of low pH and nutrient abundance. mTORC1 phosphorylates TFEB; phosphorylated TFEB binds to 14-3-3 proteins and is retained in the cytoplasm. B. TFEB is activated under lysosomal stress caused by high pH, nutrient starvation, and accumulation of intralysosomal undigested material. mTORC1 inhibition or the phosphatase calcineurin decrease the levels of phosphorylated TFEB, allowing TFEB translocation to the nucleus and inducing the expression of CLEAR network genes.

As part of the energy-sensing cascade, mTORC1 is also regulated by the AMP-dependent protein kinase (AMPK). The autophagy pathway is regulated by energy depletion through activation of the 5'-AMP activated protein kinase (AMPK), which senses cellular AMP levels. [Kim et al,2011; Mizushima et al, 2011] AMPK can activate autophagy through several mechanisms, including the direct phosphorylation of ULK1 at Ser 317 and Ser 777. [Kim et al,2011] AMPK can also phosphorylate Beclin 1 (Thr 388) leading to Vps34 activation. [Zhang et al, 2016] Depletion of cellular reducing equivalents regulates autophagy via activation of the NAD+-dependent class III histone deactylase sirtuin 1 (SIRT1). [Lee et al,2008] SIRT1 was reported to complex and catalyze the deacetylation of key autophagy regulator proteins, including ATG5, -7, -8. [Lee et al,2008]

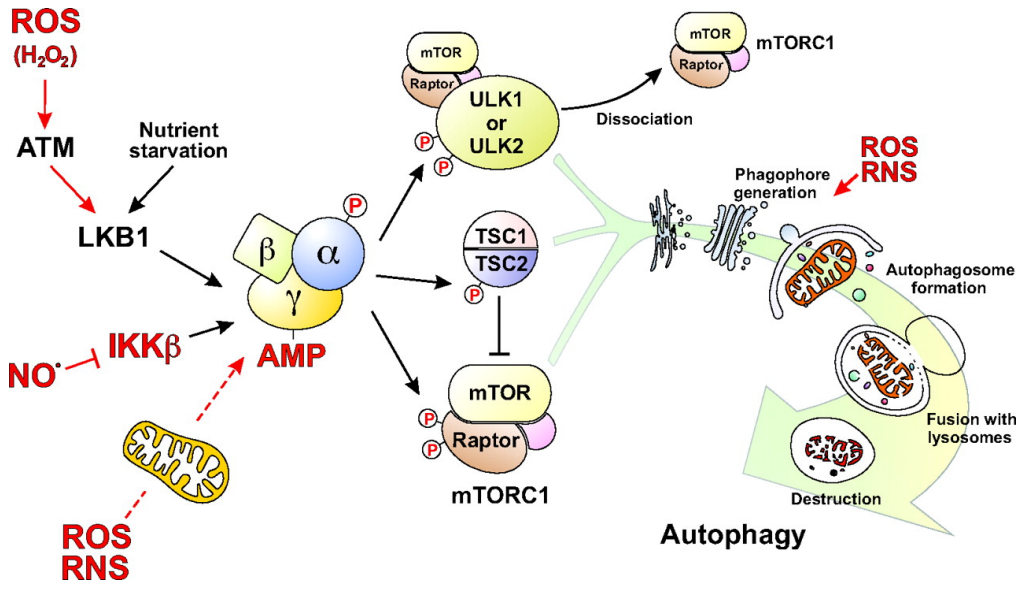

Fig4. AMPK can elicit autophagy steps by directly phosphorylating different protein substrates involved in its initiation phases.

Genetic studies have confirmed the importance of autophagy in cellular resistance to oxidative-stress and in mitochondrial maintenance. [Kara et al,2016] Secondary derangements of cellular pathways have been identified as key factors in the pathophysiology of the lysosomal storage diseases. [Lieberman et al,2012] Understanding the interrelationship between oxidative-stress and autophagy in PD, may help us design therapeutic strategies to target pathological autophagy without hindering its physiological effects.

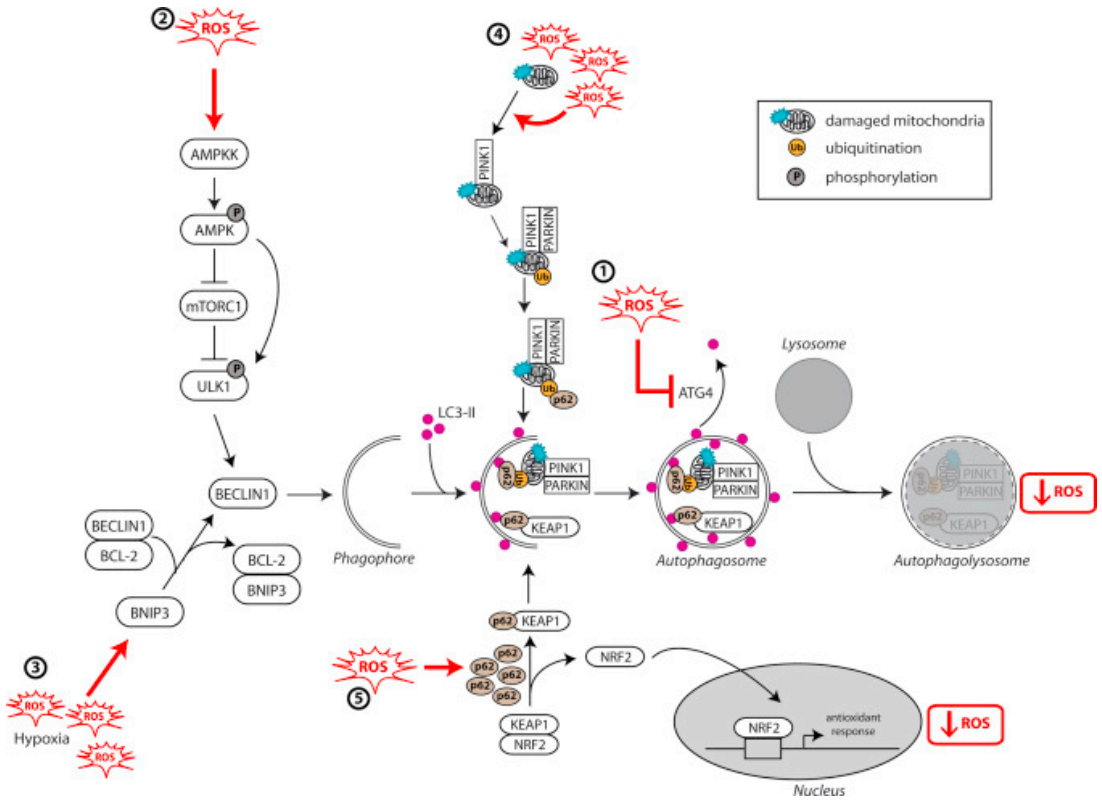

Fig5. Relationship between autophagy and ROS. ROS levels regulate autophagy levels by different pathways such as: (1) oxidization of ATG4 leading to accumulation of autophagosomes, (2) activation of the AMPK signaling cascade inducing the initiation of autophagy through the ULK1 complex, (3) disruption of BECLIN1–BCL-2 interaction leading to the initiation of autophagy or (4) alteration of mitochondria homeostasis leading to mitophagy activation. Autophagy inhibits ROS accumulation through (4) the elimination of damaged mitochondria by mitophagy or (5) the degradation of KEAP1 by selective autophagy mediated by SQSTM1/p62 and the expression of NRF2-regulated antioxidant genes.

Autophagy and oxidative-stress: The status in PD

The morphological evidence for abnormal autophagy in muscle biopsies from adult PD patients was first reported by Dr. Engel. [Kohler et al,2018] The presence of large areas of autophagic accumulation detected by electron microscopy in the therapy-resistant fast muscle suggested that abnormal autophagy might be the culprit. [Lieberman et al,2012] Surprisingly, huge clusters of LAMP1 (a lysosomal marker) and LC3 (an autophagosomal marker) positive vesicles are seen in the core of virtually every muscle fiber even in young PD mice. In humans, autophagic buildup is present in many muscle cells in late-onset patients (both juvenile and adults), thus making the observations in the mouse model relevant to the human study. [Raben et al,2010]

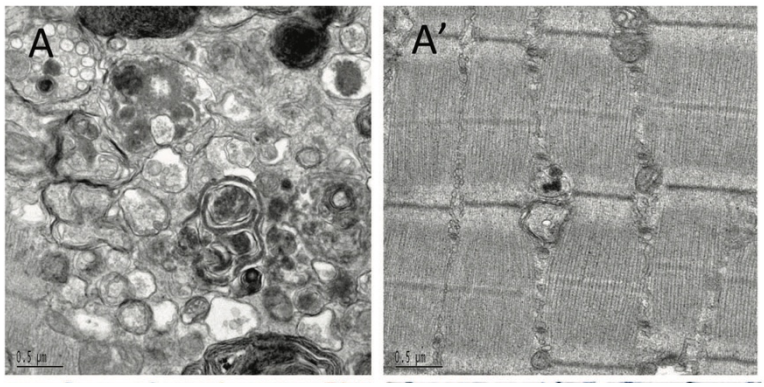

Fig6. Electron microscopy (EM) provides evidence for the presence of autophagic accumulation in the fast muscles (white part of the gastocnemius muscle) of a 5-mo-old PD knockout mouse. (A') Control.

Furthermore, it has been shown that the autophagic build-up affects the trafficking and delivery of the recombinant enzyme to the lysosome. [Fukuda et al,2006; Shea et al,2009] Thus, in PD, a profoundly disordered intracellular recycling system appears to be an important contributor to muscle weakness and incomplete response to treatment. Impaired autophagy is directly related to mitochondrial abnormalities since

damaged mitochondria are removed through the autophagic pathway, a process known as mitophagy. [Youle et al,2011] Indeed, mitochondrial alterations are observed in muscle biopsies in the majority of Pompe patients. [Schoser et al,2007] A profound dysregulation of Ca2+ homeostasis and multiple mitochondrial defects, such as a decrease in mitochondrial membrane potential, mitochondrial Ca2+ overload, an increase in reactive oxygen species, and an increase in caspase-independent apoptosis, were reported in GAA knockout (KO) mice and in primary muscle cells from PD patients. [Lim et al,2015] However, this pathway and their contribution to the pathogenesis of the disease have largely been ignored.

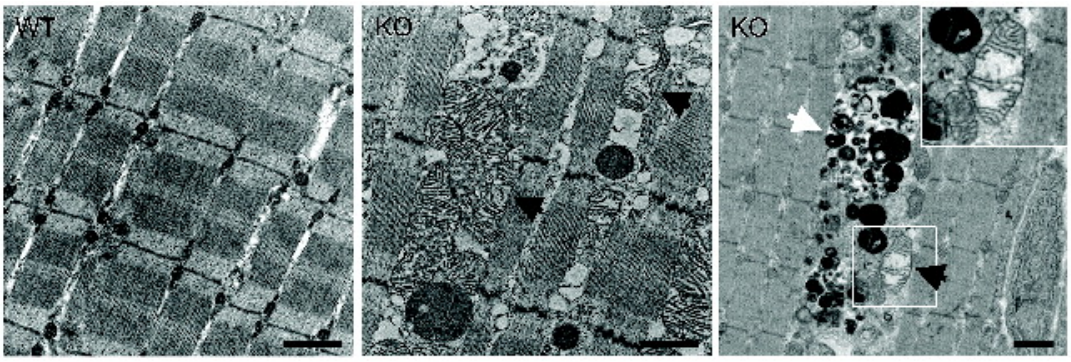

Fig7. Electron-microscopy of muscle biopsies (white part of gastrocnemius) from 5-mo-old WT and KO mice. Black arrows point to enlarged mitochondria with distorted cristae (middle and right panels and inset).

Aim of the project

The general aims of the project are to investigate the mechanisms involved in the pathophysiology of PD, since secondary abnormalities may represent novel targets of therapy. The specific aims are:

1. To characterize the oxidative-stress and autophagic pathways in vitro and in the mouse model of PD

2. Manipulate pharmacologically the oxidative-stress and autophagic pathways

RESULTS

Cultured PD patient cells and tissues from the PD mouse model show increased oxidative-stress

We evaluated the levels of oxidative-stress in PD using biochemical tests that measure ROS levels (2',7'-dichloro dihydrofluorescein, DCFDA), lipid peroxidation (Thiobarbituric Acid Reactive Substances, TBARS) and intracellular glutathione (GSH) levels and activity (5,5'-dithiobis-2-nitrobenzoic acid, DTNB). All these tests were performed on PD patients' fibroblasts and controls (Fig. 1A), on PD patients' myoblasts and controls (Fig. 1C) and on PD and WT mouse muscles (gastrocnemius, quadriceps, heart, diaphragms) and liver (Fig 1D). In all three models we considered the normal values of controls equal to 100 and we observed increased ROS levels and lipid peroxidation and reduced glutathione activity. In PD mouse, liver resulted less stressed than muscle tissues. The increase of oxidative-stress was also confirmed by western blot analyses of specific stress markers (P-Erk, P-p38 MAPK) (Fig. 1B, E). These results indicate that the oxidative-stress pathway is affected in PD, possibly contributing to the disease pathophysiology. The abnormalities found in cultured cells are representative of those found in vivo; thus, cultured cells may represent a tool for further characterization of the pathway and for drugs screenings.

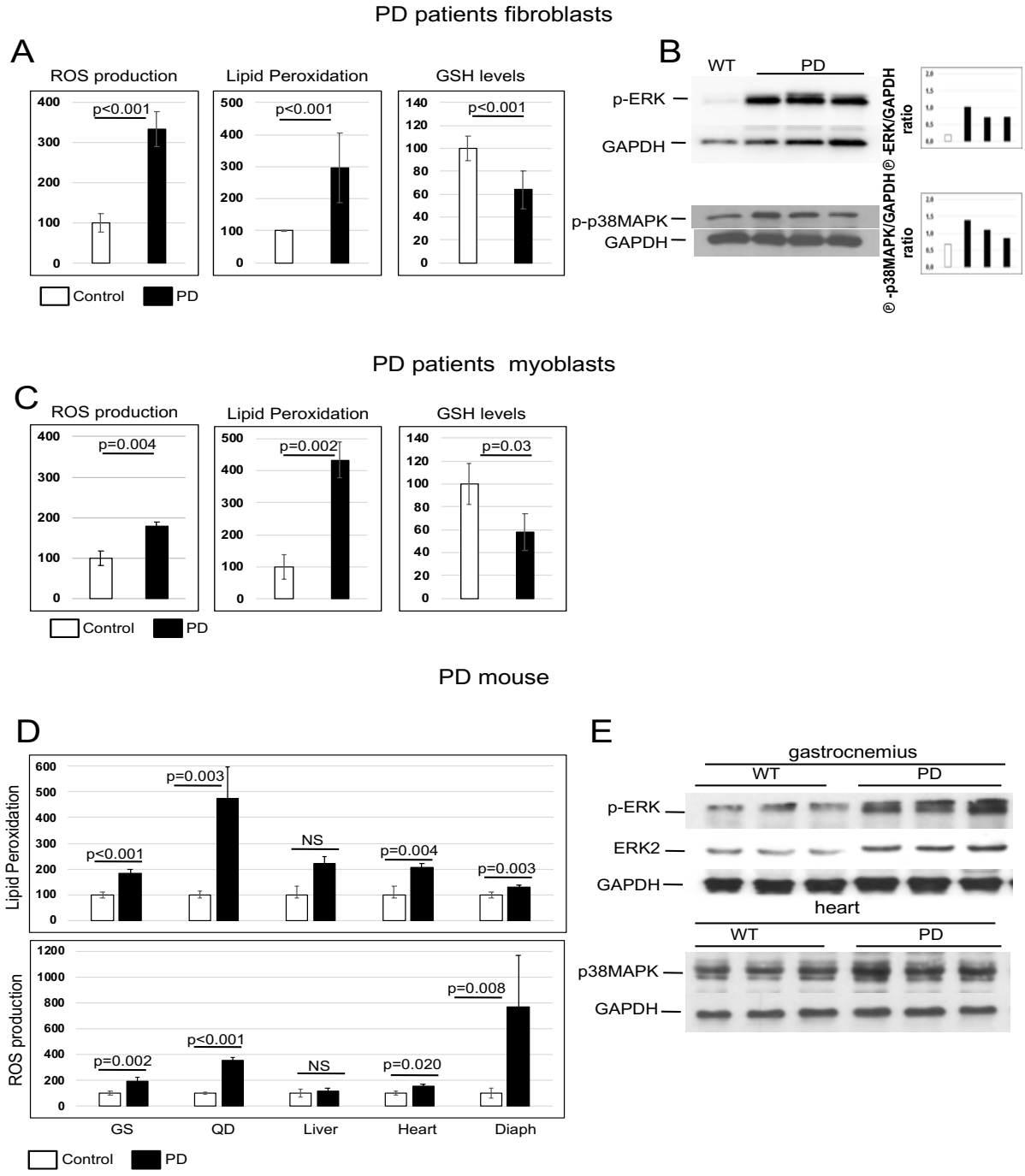

Fig1. Increased oxidative stress in PD: A, C, D) Lipid peroxidation, ROS production and GSH levels in 3 months PD mice, both fibroblasts and myoblasts isolated from patients. Lipid peroxidation levels determined by TBARS assay, intracellular ROS levels were determined by DCFDA assay, GSH levels determined by DTNB assay in WT (white bars) and in PD samples (grey bars); Data shown are the means ± S.D. of three independent experiments. B, E) Western blot analysis of P-ERK (1-2) and P38 in WT and PD fibroblasts and in different tissue from mouse model.

Oxidative-stress is related to the impairment of the autophagic pathway

To better evaluate the hypothesis that oxidative-stress is a consequence of autophagy, we physiologically or pharmacologically activated autophagy. As shown in Fig.2, we used starvation (for 4h), rapamycin (20μM for 24h), a known inhibitor of the mTOR complex, and MK6-83 and MLSA-1 (30μM for 24h), two known activators of Mucolipin TRP channel 1 (TRPML1) a lysosomal Ca2+ channel. In all instances activation of autophagy resulted into reduced levels of oxidative-stress, as shown by reduced ROS levels and lipid peroxidation and increased GSH activity. When we inhibited autophagy by Bafilomycin, a V-ATPase inhibitor, we obtained opposite effect with a further increase of oxidative-stress. These results indicate that the impairment of autophagy is one of the factors implicated in oxidative-stress in PD, and that activation of autophagy may represent a strategy to reduce cellular stress.

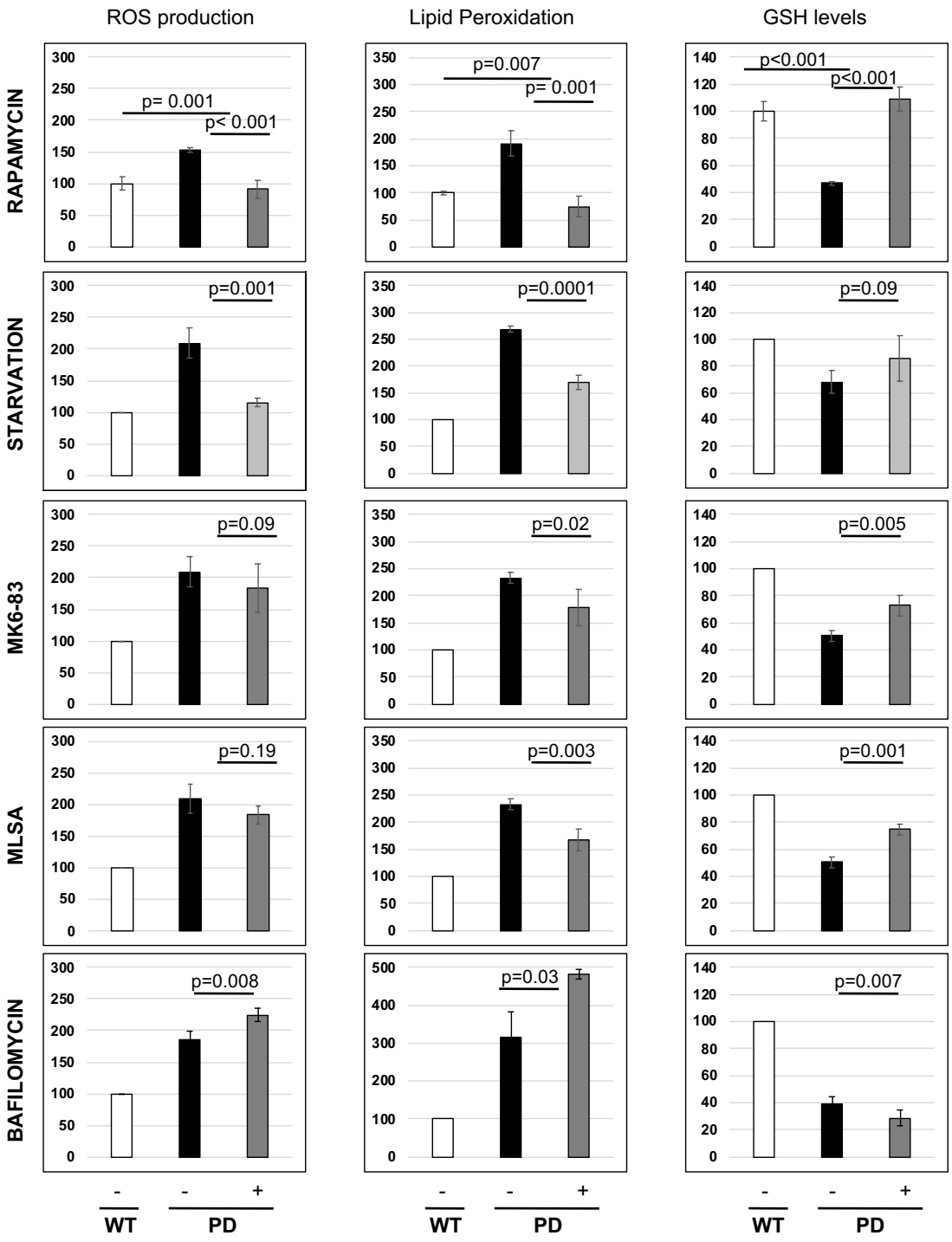

Fig2. Modulation of autophagy impacts on stress in fibroblasts: Lipid peroxidation, ROS production and GSH levels in fibroblasts isolated from patients. WT (white bars), PD samples (black bars) and PD treatment (grey bars); Data shown are the means ± S.D. of three independent experiments.

Stress impacts on the uptake of the recombinant enzyme (rhGAA) used for ERT

Previous literature suggests that oxidative-stress affects the function of clathrin-mediated endocytosis. [Volpert et al, 2017] We sought for possible correlation between oxidative-stress and the response to ERT by in-vitro experiments. We treated six PD fibroblasts cell lines with rhGAA to see their ability to internalize the exogenous enzyme of ERT comparing to stress level of each one. We found inverse correlations between the levels of single stress indicator and correction of GAA activity by rhGAA (Fig. 3A, B, C); more evident in lipid peroxidation and ROS levels. By combining the results of the three tests in each single patient cells, we calculated a cumulative “stress score” and the inverse correlation coefficient was highly significant (-0.99) (Fig. 3D). This means that higher levels of oxidative-stress found in patients correspond to decreased ability to respond to therapy and indicates that increased oxidative-stress may have deleterious effects on the efficacy of enzyme replacement therapy in PD.

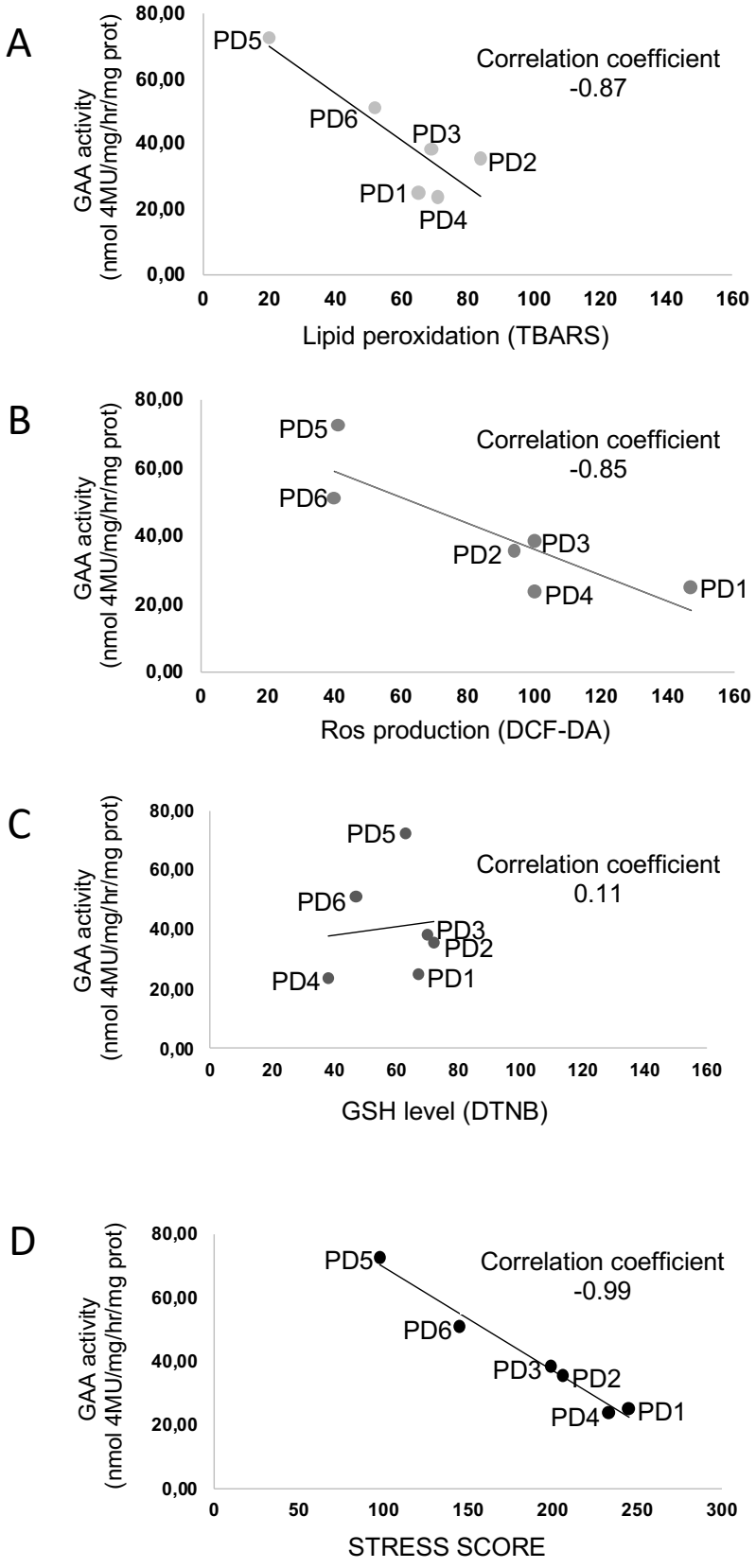

Fig3. Stress impacts on correction of GAA activity by ERT: The correlations between the levels of stress indicators and correction of GAA activity by rhGAA.

Induction of oxidative-stress with sodium arsenite affects rhGAA uptake/processing

To further support our idea that stress could impact the efficacy of the therapy we induced additional stress in patients' cells and we looked again at the internalization of rhGAA. As expected, treatment with sodium arsenite 100μM for 4h induced further increase of ROS level and lipid peroxidation, reduced level of GSH (Fig. 4A) and increased of P-p38MAPK (Fig. 4B). The ability of rhGAA internalization was assessed under these conditions (Fig. 4D). GAA activity was significantly reduced both at 6 hours and at 24 hours, as also shown by western blot analysis of GAA that showed impaired processing of the GAA precursor in to the mature 76-70 kDa active isoforms in the presence of arsenite.

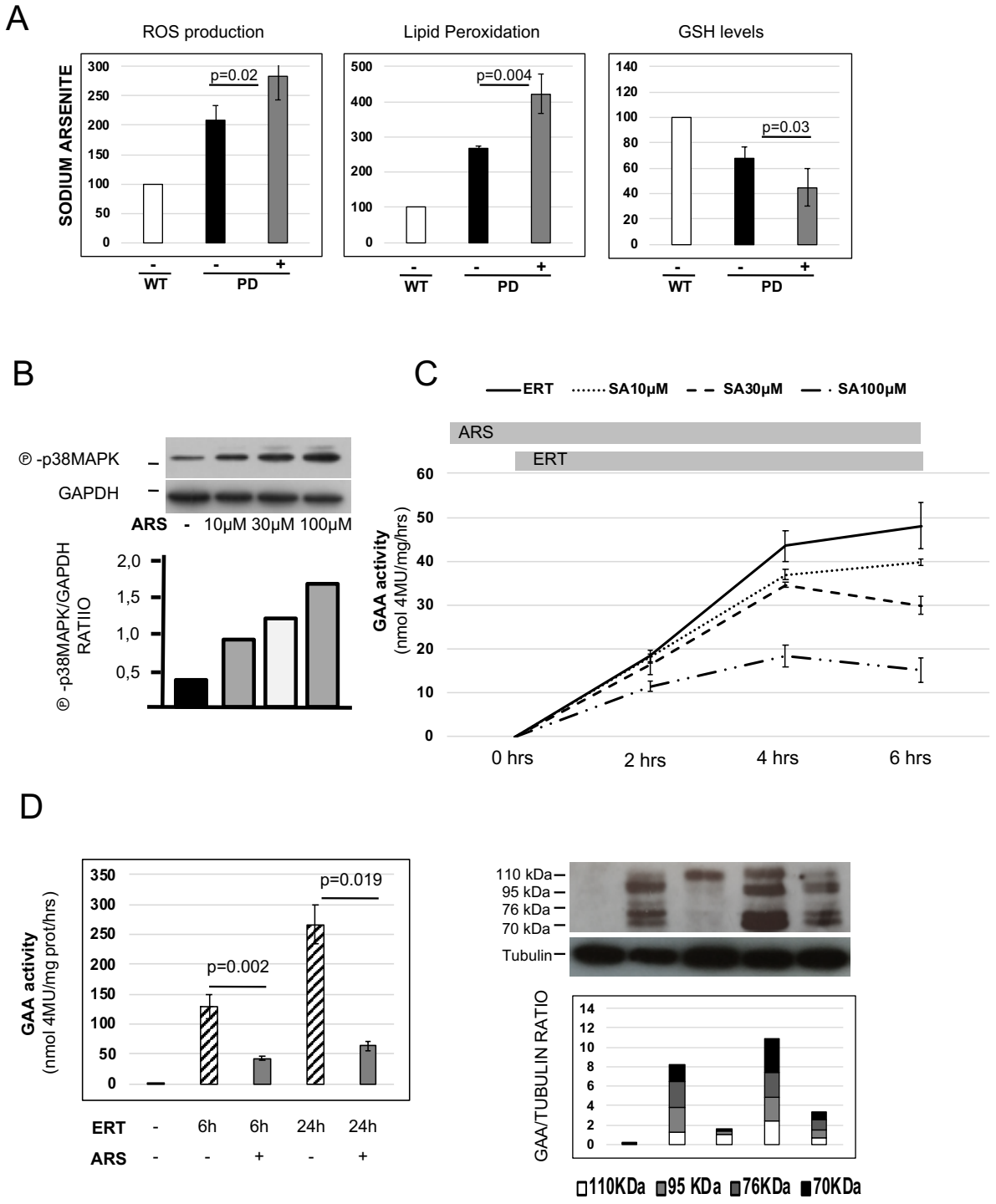

Fig4. Induction of oxidative stress with sodium arsenite affects rhGAA uptake/processing: A) Lipid peroxidation, ROS production and GSH levels in fibroblasts isolated from patients after a 4 hours treatment with sodium arsenite. WT (white bars), PD samples (black bars) and PD treatment (grey bars); B) Western blot analysis of P38 in PD fibroblasts after a 4 hours treatment with sodium arsenite a different concentrations; C,D) Percent of GAA activity increasing in PD fibroblasts treated with ERT with and without sodium arsenite D) Western Blot analysis of GAA isoforms and quantitative analysis of the different enzyme isoforms.

Antioxidants improve rhGAA uptake and processing

On the basis of literature data, we selected some molecules that are known to have an antioxidant effect. We used Idebenone (IDE), Edaravone (EDA), N-AcetylCysteine (NAC) and Resveratrol (RESV). As expected, antioxidants reduced significantly stress levels measured by TBARS, DCF-DA, and DTNB in PD fibroblasts (Fig. 5). Co-incubation for 24 hrs of rhGAA with antioxidant drugs resulted in improved correction of GAA activity (FIGURE 6a), increased amounts of GAA-related polypeptides on western blot analysis, and enhanced processing of the rhGAA 110 kDa polypeptide into the mature 76-70 kDa active isoforms (Fig. 6B), indicating improved uptake trafficking of the recombinant enzyme to lysosomes.

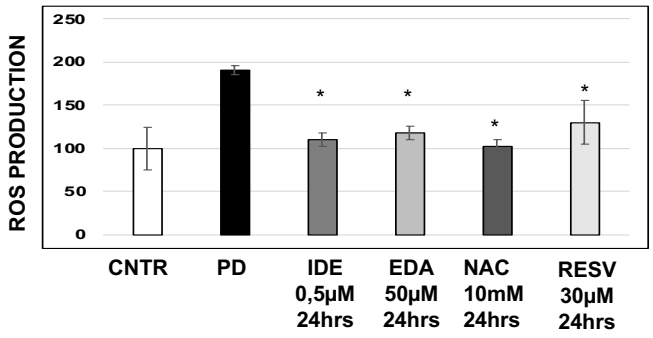

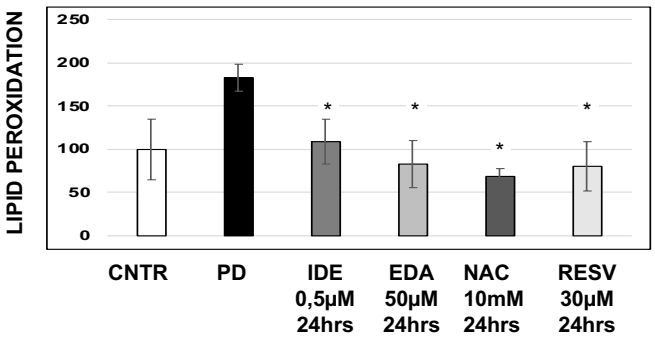

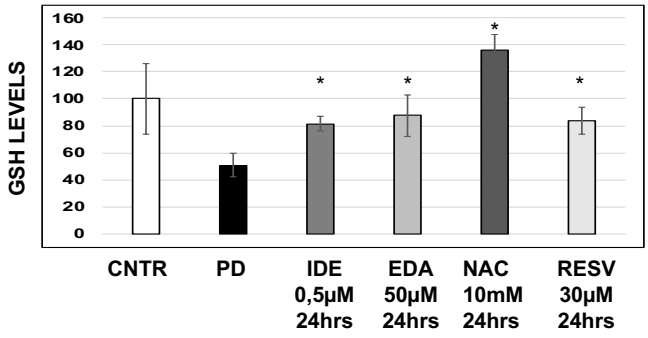

Fig5. Effect of antioxidants on stress: Lipid peroxidation, ROS production and GSH levels in fibroblasts isolated from patients after a treatment with different antioxidants. * All statistically significant ($p < 0.001$) compared to untreated PD.

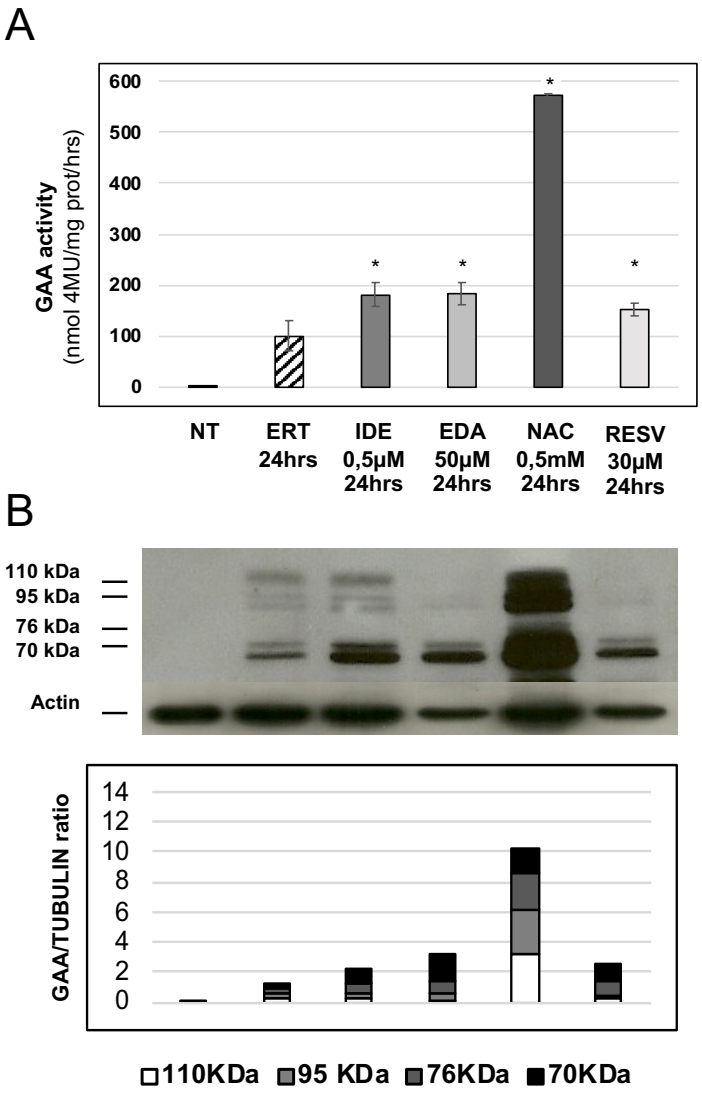

Fig6. Effect of antioxidants on ERT: A) Percent of GAA activity increasing in PD fibroblasts treated with ERT with and without antioxidants. B) Western Blot analysis of GAA isoforms and quantitative analysis of the different enzyme isoforms. * All statistically significant ($p < 0.05$) compared to treated with ERT alone.

The antioxidants improve MPR recycling in PD fibroblasts

A possible factor that could explain the improvement of rhGAA uptake and processing is the effect of antioxidants on the trafficking and localization of the mannose-6-phosphate receptor (MPR). Cells were incubated in the presence of an anti-MPR antibody at 16^{o} C for 1h in order to synchronize MPR trafficking. After switching the temperature to 37^{o} C, MPR trafficking was followed at different time points (15 min, 30 min) by immuno-fluorescence analysis. MPR trafficking was impaired in PD cells compared to controls. In the presence of antioxidants, idebenone and NAC, PD fibroblasts showed improved MPR trafficking, comparable to that seen in control cells at 30 min (Fig. 7) and co-localization with the trans-Golgi marker TGN46, suggesting that correction of stress improves trafficking of membranes and membrane-bound proteins. The improved MPR localization and trafficking is likely to contribute to the enhancement of rhGAA uptake and trafficking.

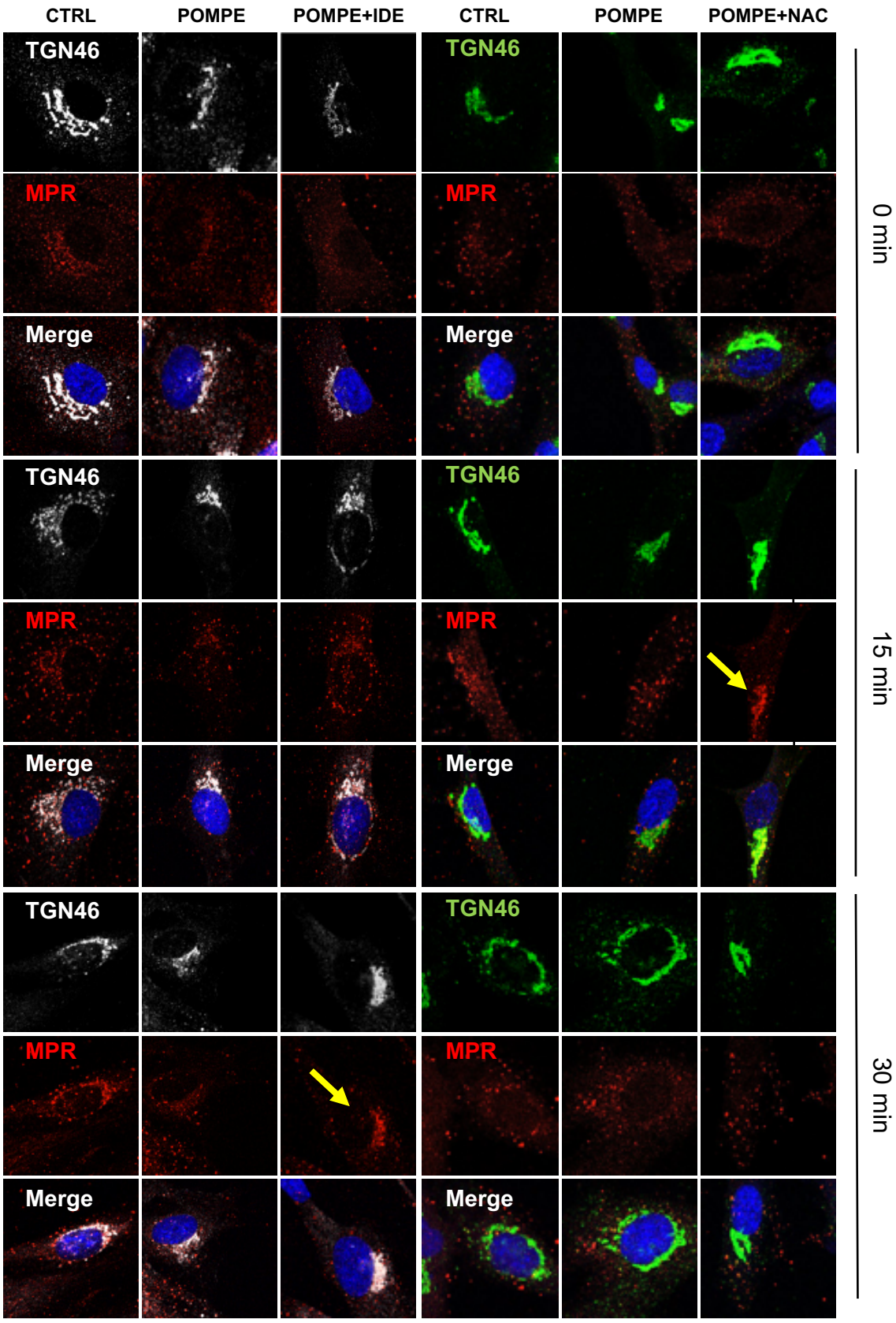

Fig7. Effect of antioxidants on MPR localizazion: Immunofluorescence analysis of CI-MPR distribution and TGN46 in control and fibroblasts patients by confocal fluorescence microscopy. Fibroblasts treated with and without antioxidants at different time points.

Modulation of autophagy impacts on ERT

We showed that modulation of autophagy has an effect on stress reduction (Fig. 2). We therefore tested the effect of activation of autophagy on ERT uptake. Co-incubation for 24 hrs of rhGAA with drugs resulted in improved correction of GAA activity (Fig. 8A), increased amounts of GAA-related polypeptides on western blot analysis, and enhanced processing of the rhGAA 110 kDa polypeptide into the mature 76-70 kDa active isoforms (Fig. 8B), indicating improved uptake trafficking of the recombinant enzyme to lysosomes.

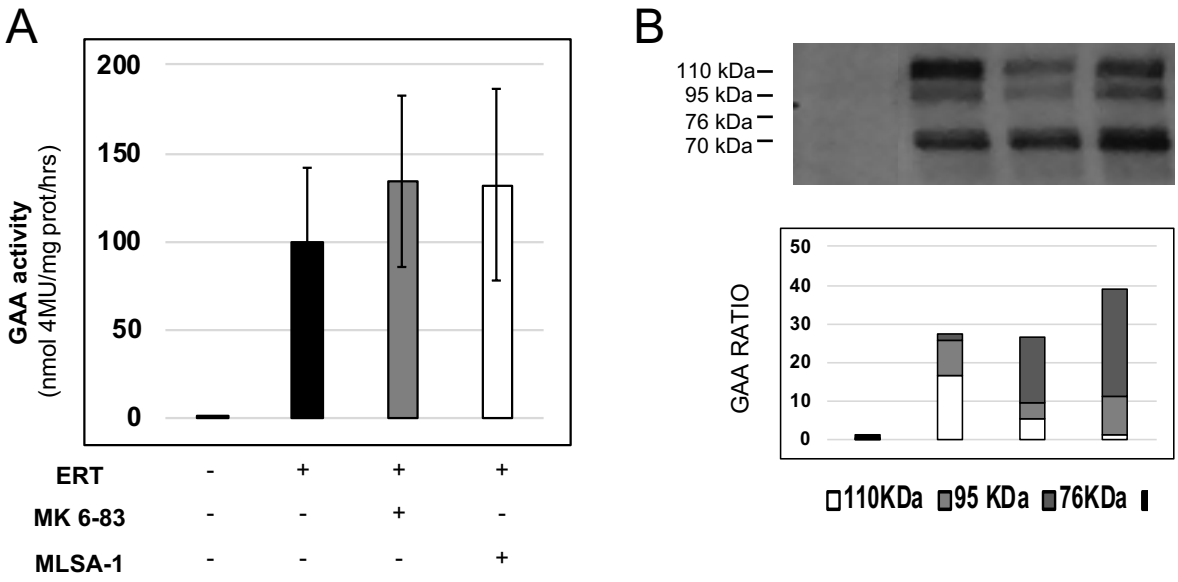

Fig8. Modulation of autophagy impacts on ERT: A) Percent of GAA activity increasing in PD fibroblasts treated with ERT with and without drugs. B) Western Blot analysis of GAA isoforms and quantitative analysis of the different enzyme isoforms.

A pilot study- The antioxidant n-acetylcysteine enhances enzyme replacement therapy with rhGAA and glycogen clearance in vivo

Treatment of mice with n-acetylcysteine (2gr/day by gavage) 24 hrs before and on the day of a single intravenous injection of 40 mg/kd rhGAA resulted into improved levels

of tissue GAA activity in tissues, compared to mice treated with rhGAA alone (Fig. 9A). In quadriceps and diaphragm the increase reached statistical significance (p=0.01 and 0.001, respectively). GAA activity in diaphragm, a critical muscle for respiratory function, attained levels that are close to those found in control mice (shaded area). Co-dosing of n-acetylcysteine and a single intravenous injection of 100mg rhGAA resulted into an enhanced glycogen clearance from tissues (Fig. 9B). These results suggest that protocol based on the combination of antioxidant and enzyme replacement therapy may translate into improved exposure of tissues to the therapeutic enzyme and better clearance of the stored substrate.

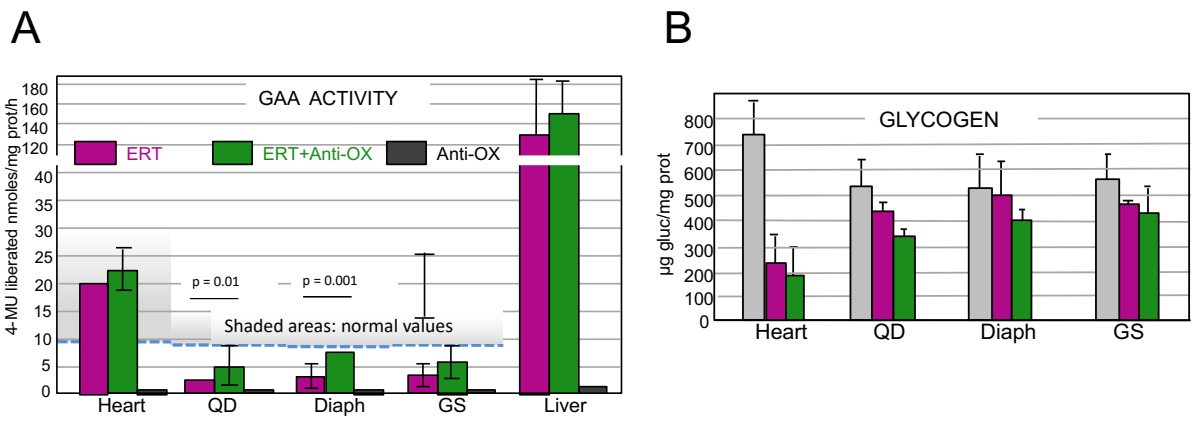

Fig9. Effect of antioxidants in PD mouse: A) In all tissues examined (liver, heart, diaphragm, and gastrocnemium) the combination of NAC and rhGAA (green bars) resulted in higher GAA enzyme activity compared to rhGAA and NAC alone (pink and grey bars); B) Glycogen content was evaluated in gastrocnemius (GS), quadriceps (QD), diaphragm (Diaph) and heart of PD mouse, ERT-treated and ERT-NAC.

New therapeutic pathaway for lysosomal storage diseases?

Secondary cellular abnormalities are now recognized as major players in the pathogenetic cascade of LSDs and may affect the efficacy of therapies. In preliminary, exploratory studies we evaluated the status of the autophagic and oxidative-stress pathways also in cultured Mucopolysaccharidosis Type IV A (MPSIVA) fibroblasts. The results obtained indicate that also in MPSIVA autophagy is affected and that oxidative-stress is increased. In MPSIVA fibroblasts we found an increase of LC3-II and p62 levels (Fig. 10B). In addition, we found a significant increase in lipid peroxidation, ROS levels and intracellular GSH levels (Fig. 10A). p38-MAPK phosphorylation was also substantially increased. We used autophagy-modulating drugs, as described for PD, enhance ERT. Co-incubation for 24 hrs of rhGALNS with drugs increased amounts of GALNS-related polypeptides on western blot analysis, and enhanced processing of the rhGALNS 55kDa polypeptide into the mature 40kDa active isoform (Fig. 11), indicating improved uptake trafficking of the recombinant enzyme to lysosomes. The results confirm that the oxidative and the autophagic-lysosomal pathways are impaired in LSDs, and that these pathways may be manipulated in order to enhance the efficacy of approved therapies, such as enzyme replacement therapy.

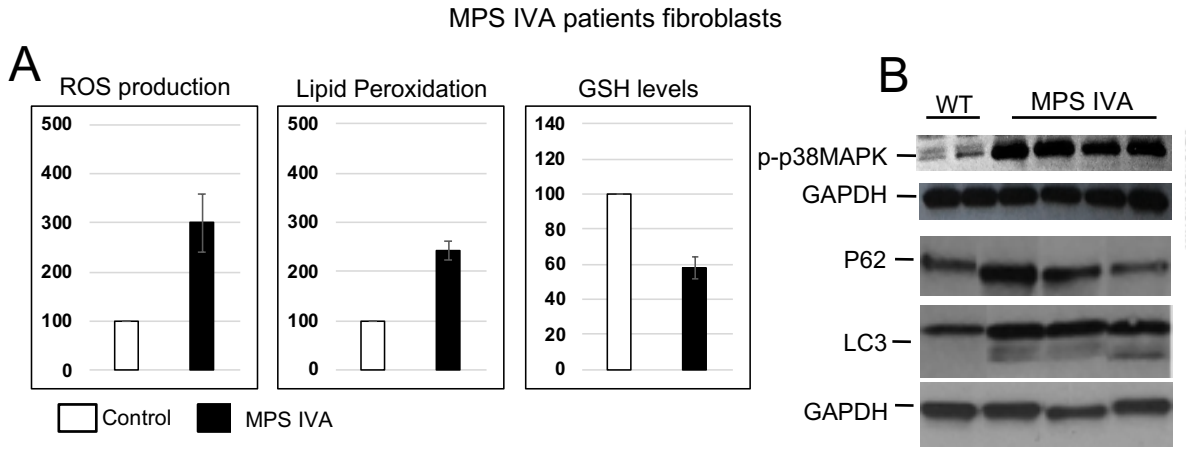

Fig10. **Increased oxidative stress in MPSIVA**: A) Lipid peroxidation, ROS production and GSH levels in fibroblasts isolated from patients. WT (white bars) and in MPSIVA samples (grey bars); B) Western blot analysis of P38, P62 and LC3 in WT and MPSIVA fibroblasts.

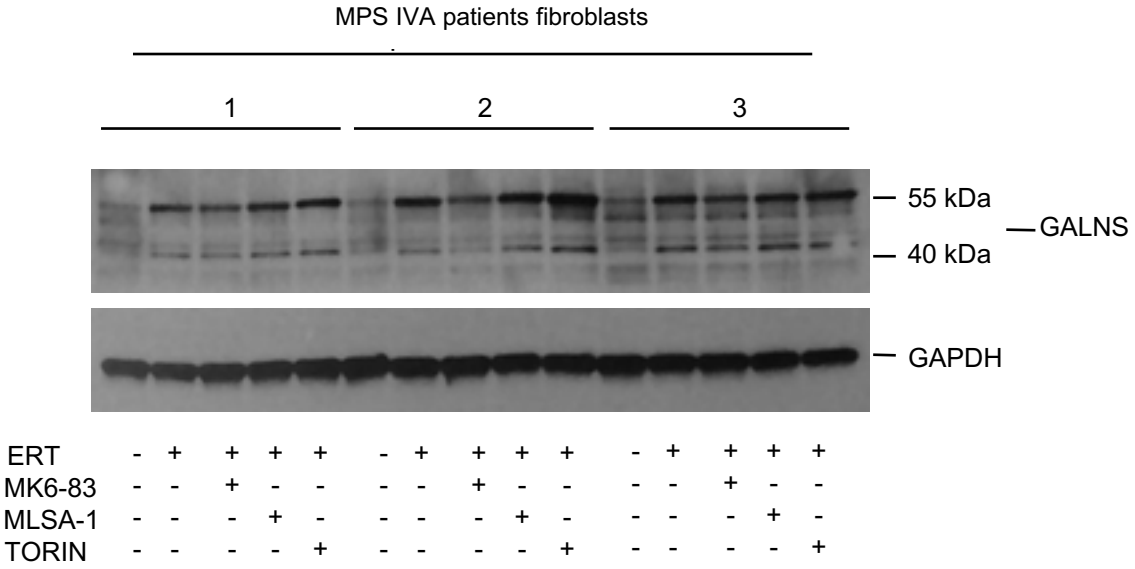

Fig11. **Modulation of autophagy impacts on ERT:** Western Blot analysis of GALNS isoforms in MPSIVA fibroblasts treated with ERT with and without drugs.

CONCLUSIONS

PD pathophysiology and its molecular/cellular mechanisms are not fully understood. Glycogen storage in cells and tissues and impairment of autophagy have been well characterized, however other secondary abnormalities of cellular pathways need further characterization. This is particularly important since secondary abnormalities may represent novel targets of therapy. In fact, albeit highly effective on some aspects of PD (reversal of cardiac involvement and prolonged survival in classic infantile-onset patients; improved or stabilized neuromuscular deficits and respiratory function in late-onset patients), current therapies for PD show important limitations. The aims of my thesis were to better characterize the secondary dysregulation of cellular pathways triggered by storage in PD, and to investigate whether these abnormalities may represent novel therapeutic targets, complementary to existing therapies. We have performed a thorough characterization of the oxidative-stress and autophagic pathways in PD cells (both fibroblasts and myoblasts) and in tissues from the murine model of the disease. Cell studies were done under basal conditions and under stress condition. In addition, we have studied the consequences of increased oxidative-stress on the uptake and trafficking of rhGAA. Finally, we studied drugs that modulate oxidative-stress ad autophagy and their effects as a complementary approach in combination with ERT (modulation of stress, enzyme correction, enzyme processing effects on the recycling of the MPR). Our results provide the proof of concept that correcting secondary abnormalities in PD cells may enhance uptake and processing of the recombinant enzymes used for enzyme replacement therapy, possibly with a synergistic effect. Most of the small-molecules that we tested in this research are approved for human therapy (such as antioxidants). Should our preclinical studies prove successful, the translation into clinical trial(s) could be immediate and improve patients' quality of life.

Materials and methods

Patients' fibroblst and animal model

A KO PD mouse model obtained by insertion of neo into the GAA gene exon 6 Raben et al, [1998] was purchased from Charles River Laboratories (Wilmington, MA), and is currently maintained at the Cardarelli Hospital's Animal Facility (Naples, Italy). Animal studies were performed according to the EU Directive 86/609, regarding the protection of animals used for experimental purposes. Every procedure on the mice were performed with the aim of ensuring that discomfort, distress, pain, and injury would be minimal. Mice were euthanized following anesthesia. Human PD fibroblasts (approximately 30 cell lines) are already available at the cell bank of the Department of Translational Medical Sciences (DISMET), Section of Pediatrics, Federico II University, Naples. Fibroblasts were grown in Dulbecco's modified Eagle's medium (Invitrogen, NY, USA), supplemented with 20% fetal bovine serum (Invitrogen, NY, USA), 2 mM L-glutamine, and antibiotics (Invitrogen, NY, USA). Cells were grown in a 5% CO_2 humidified atmosphere at 37 °C.

Gaa activity assay

GAA activity was assayed by using the fluorogenic substrate 4- methylumbelliferyl-alpha-D galactopyranoside (Sigma-Aldrich). Fibroblasts were harvested by trypsinization and disrupted by freezing and thawing (3X). Cell homogenates (10μg of protein) were incubated at 37° for 60 min with 2mM 4-methylumbelliferyl a-D-glucopyranoside as substrate in a 0.2 acetate buffer pH 4.0 in an incubation mixture of 20μl. Reactions were stopped with 1 ml glycine carbonate buffer pH 10.7 and fluorescence was read on a Turner biosystems fluorometer Modulus 9200 (360nm

excitation, 450nm emission). Protein concentration in cell homogenates was measured according to Lowry method.

Cell lysates

Cells were plated at a density of $3x10^4$ cells/cm^2 in DMEM + 20% FBS (Invitrogen, NY, USA), + 2 mM L-glutamine (Invitrogen, NY, USA), and antibiotics for 24 h at 37°C. The cells were washed with PBS and detached by trypsinization, and centrifuged at 10,000 rpm at RT. The cell pellets were resuspended in RIPA buffer with addiction of protease inhibitor cocktail (Roche Diagnostics, Mannheim, Germany) and phosphatase inhibitor, and incubated on ice, by vortexing every 5 minutes. Upon 30 min incubation on ice, lysates were centrifuged at 14,000 g for 30 min at 4°C. Following the Lowry assay, reported above, aliquots of 20 µg of cytosolic proteins were separated on a 15% SDS-PAGE, and Western blotting analyses were performed.

Mice tissue lysates

Mice tissue protein extracts were obtained by lysing cells with RIPA buffer and with addiction of protease inhibitor cocktail (Roche Diagnostics, Mannheim, Germany) and phosphatase inhibitors for 3 minutes at 50 oscillations/minute in tissue lyser (Qiagen, Hilden, Germany) and by five cycles of freeze-thawing. Samples were centrifuged at 14,000 g for 30 minutes at 4°C. Following the Lowry assay, reported above, aliquots of 20µg of cytosolic proteins were separated on a 15% SDS-PAGE, and Western blotting analyses were performed.

Western Blot

Sodium dodecyl sulfate polyacrylamide gel electrophoresis (SDS-PAGE) was performed as described by Laemmli using 15% polyacrilamide gel in a vertical slab gel

apparatus. Reduced loading buffer (0.125 M Tris-HCl pH 6.8 containing 2% SDS, 10% glycerol, 0.02% bromophenol blue and 5% 2-mercaptoethanol) was added to protein samples. The mixture was boiled for 2 minutes, centrifuged and loaded on the gel. Following gel electrophoresis, proteins were transferred on polyvinylidene fluoride (NC membranes, Amersham, Freiburg, Germany) (100V, 1h, at 4°C). Membranes were then incubated with the blocking solution (5% BSA or MILK 5% in TBS buffer containing 0.1% Tween-20) at room temperature for 30min. Following blocking step, membranes were washed with TBS buffer containing 0.1% Tween-20 (TBS-T) , and incubated at RT for 1h with anti-phospho p38 antibody (Cell Signaling, Danvers, MA, USA; 1:1000 diluition), anti-phospho pERK antibody (Cell Signaling, Danvers, MA, USA; 1:1000 diluition), anti-ERK2 antibody (Cell Signaling, Danvers, MA, USA; 1:1000 diluition), anti-GALNS antibody (Themofisher, Thermo Scientific, Rockford, IL; 1:1000 diluition)in 2,5% BSA in TBS-T; anti-GAA antibody (PRIMM; 1:500 diluition), anti-GAPDH antibody (Ambion, Austin. TX, USA; 1:10000 diluition), anti-actin antibody (Sigma-Aldrich, St. Louis, MO, USA; 1:1000 diluition), anti-tubulin antibody (Sigma-Aldrich, St. Louis, MO, USA; 1:1000 diluition), anti-LC3 antibody (Novus Biologicals, Abingdon, UK; 1:500 diluition)), anti-P62 antibody (Sigma-Aldrich, St. Louis, MO, USA; 1:1000 diluition) in 2,5 % MILK in PBS buffer containing 0.1% Tween-20 (PBS-T). Membranes were then washed with TBS-T and incubated on a shaker for 1h at room temperature with goat anti-rabbit or goat anti-mouse secondary antibodies conjugate to horseradish peroxidase enzyme (HRP). Membranes were then washed with TBS-T. The detection of immuno-positive species by enzyme-linked chemiluminescence (enhanced chemiluminescence: ECL) was performed according to the manufacturer's instructions (ECL, Amersham, Freiburg, Germany), Quantitative analysis of band intensity was performed using ImageJ or using a Phosphoimager (Biorad).

DTNB assay

The interaction of the sulfhydryl group of GSH with 5,5′-dithiobis- 2-nitrobenzoic acid (DTNB) produces a yellow-coloured compound, 5-thio-2-nitrobenzoic acid (TNB), whose intensity can be measured at 412 nm. Thus, the rate of TNB production is directly proportional to the concentration of GSH in the sample. To estimate intracellular GSH levels, cells were detached by trypsin, centrifuged at 1000×g for 10min and re-suspendend in RIPA buffer, containing protease inhibitors. After 30 min incubation on ice, lysates were centrifuged at 14,000×g for 30 min at 4 ◦C. Supernatant protein concentration was determined by the Lowry assay. Then 50µg of proteins were incubated with 3 mmol $L^{-}1$ ethylenediaminetetraacetic acid (EDTA) and 144 µmol $L^{-}1$ DTNB in 30 mmol $L^{-}1$ Tris HCl (pH 8.2) and centrifuged at 14,000×g for 5min at room temperature. Finally, the absorbance of the supernatant was measured at 412 nm using a multiplate reader (Epoch Biotek. Winooski,USA). GSH levels were expressed as percentage of TNB absorbance of the sample under test compared with the untreated sample. Three separate analyses were carried out with each extract.

DCFDA assay

To determine ROS levels within the cytosol, cells were incubated with the cell permeable redox-sensitive fluorophore 2′ ,7′ -dichlorodihydrofluorescein diacetate (H2 -DCFDA) (Sigma-Aldrich) at a concentration of 25 µmol $L^{-}1$ for 30 min at 37 ◦C. Cells were then washed twice with warm phosphate-buffered saline(PBS) supplemented with 1 mmol $L^{-}1$ $CaCl_2$, 0.5 mmol $L^{-}1$ $MgCl_2$ and 30 mmol $L^{-}1$ glucose (PBS plus), detached by trypsin, centrifuged at 1000g for 10 min and re-suspended in PBS plus at a density of 1×10^5 cellsm$L^{-}1$. H_2-DCFDA is non-fluorescent until, in the presence of ROS, it is hydrolysed by intracellular esterases and readily oxidized to the highly fluorescent 2′ ,7′-dichlorofluorescein (DCF). DCF fluorescence intensity was measured

at an emission wavelength of 525 nm and an excitation wavelength of 488 nm using a PerkinElmer LS50 spectrofluorimeter. Emission spectra were acquired at scanning speed of 300 nm min^{-1}, with five slit widths for excitation and emission. ROS production was expressed as percentage of DCF fluorescence intensity of the sample under test compared with the untreated sample. For homogenate from tissues were assayed as described above. Three separate analyses were carried out with each extract.

Measurement of Lipid Peroxidation

The levels of lipid peroxidation were determined by using the thiobarbituric acid reactive substances (TBARS) assay. Briefly, cells were detached by trypsin, centrifuged at 1000g for 10min and 5×10^5cells were re-suspendend in 0.67% thiobarbituric acid (TBA) and an equal volume of 20% trichloroacetic acid was added. The samples were then heated at 95 °C for 30 min, incubated on ice for 10 min and centrifuged at 3000g for 5 min, at 4°C. TBA reacts with the oxidative degradation products of lipids in samples, yielding red complexes that absorbance at 532 nm. Lipid peroxidation levels were expressed as percentage of absorbance at 532 nm of the sample under test, compared to the untreated sample. For homogenate from tissues were assayed as described above. Three independent experiments were carried out, each one with three determinations.

Immunofluorescence studies

To study the distribution of CI-MPR, human fibroblasts grown on coverslips were fixed using PFA 4% and blocked with 0.05% saponin, 5% BSA, 50mM NH_4Cl, 0,02% NaN_3 diluted in PBS for 1 hour. The cells were incubated with the primary antibodies, with secondary antibodies in blocking solution and then mounted with vectashield mounting medium with DAPI (Vector Laboratories, Burlingame, CA).

For experiments shown, images were taken using a Zeiss LSM700 confocal microscope (Carl Zeiss, Jena, Germany) integrated with the AxioCam MR camera and 63x oil objective. Digital images were captured by using Zeiss AxioVision software and maximum intensity projections were generated using Image J software. Results of these analyses were obtained on a total of 100 cells for each cell line.

Glycogen assay

Glycogen concentration was assayed in tissue lysates by measuring the release of glucose after digestion with Aspergillus niger amyloglucosidase (Sigma Aldrich, Saint Louis, MO, USA). Data were expressed as µg of glycogen/mg of protein.

Chapter 2

microRNA AS BIOMARKES IN PD

INTRODUCTION

Enzyme replacement therapy (ERT) with recombinant human GAA (rhGAA) is presently the only approved pharmacologic treatment to PD. [Van den Hout et al, 2000] The patients' response to ERT is highly variable. Although extraordinarily effective in some patients and on some aspects of the disease (most notably survival and cardiomyopathy in infantile patients; motor and respiratory function in late-onset forms), in other patients ERT results in minor effects in specific muscles with signs of continuing disease progression. [Prater et al, 2012] A major issue in the monitoring of disease stage and therapeutic efficacy is the availability of objective and reliable tests that are not influenced by inter and intra-investigator variance. Currently, clinical tests (muscle strength, muscle function, patient-reported outcomes) are in common use. [Angelini et al,2012] The aim is to identify new reliable biomarkers to monitor of disease progression and of efficacy of therapies, and to obtain information on the pathophysiology of PD. We explored the possibility to use microRNAs (miRNAs) as disease markers in PD.

ARTICLE | Genetics inMedicine

microRNAs as biomarkers in Pompe disease

Antonietta Tarallo, PhD[1,2], Annamaria Carissimo, PhD[2,3], Francesca Gatto, PhD[2], Edoardo Nusco, BS[2], Antonio Toscano, MD[4], Olimpia Musumeci, MD[4], Marcella Coletta, PhD[1,2], Marianthi Karali, PhD[2,5], Emma Acampora, MD[1], Carla Damiano, BS[1,2], Nadia Minopoli, BS[1], Simona Fecarotta, PhD[1], Roberto Della Casa, MD[1], Tiziana Mongini, MD[6], Liliana Vercelli, MD[6], Lucio Santoro, MD[7], Lucia Ruggiero, MD[7], Federica Deodato, MD[8], Roberta Taurisano, MD[8], Bruno Bembi, MD[9], Andrea Dardis, PhD[9], Sandro Banfi, MD[2,5], WW Pim Pijnappel, PhD[10], Ans T van der Ploeg, PhD[10] and Giancarlo Parenti, MD[1,2]

Purpose: We studied microRNAs as potential biomarkers for Pompe disease.

Methods: We analyzed microRNA expression by small RNA-seq in tissues from the disease murine model at two different ages (3 and 9 months), and in plasma from Pompe patients.

Results: In the mouse model we found 211 microRNAs that were differentially expressed in gastrocnemii and 66 in heart, with a different pattern of expression at different ages. In a preliminary analysis in plasma from six patients 55 microRNAs were differentially expressed. Sixteen of these microRNAs were common to those dysregulated in mouse tissues. These microRNAs are known to modulate the expression of genes involved in relevant pathways for Pompe disease pathophysiology (autophagy, muscle regeneration, muscle atrophy). One of these microRNAs, miR-133a, was selected for further quantitative real-time polymerase chain reaction analysis in plasma samples from 52 patients, obtained from seven Italian and Dutch biobanks. miR-133a levels were significantly higher in Pompe disease patients than in controls and correlated with phenotype severity, with higher levels in infantile compared with late-onset patients. In three infantile patients miR-133a decreased after start of enzyme replacement therapy and evidence of clinical improvement.

Conclusion: Circulating microRNAs may represent additional biomarkers of Pompe disease severity and of response to therapy.

Genetics in Medicine (2019) 21:591–600; https://doi.org/10.1038/s41436-018-0103-8

Keywords: Pompe disease; microRNAs; miR-133a; Enzyme replacement therapy; Next-generation sequencing

INTRODUCTION

Pompe disease (glycogenosis type 2, OMIM 232300, ORPHA365, ICD-10 E74.0) is a metabolic myopathy caused by pathogenic variants of the *GAA* gene and deficiency of acid α-glucosidase (GAA), an enzyme involved in the lysosomal breakdown of glycogen.[1] The primary pathological hallmarks of Pompe disease are generalized glycogen storage, most prominent in heart and skeletal muscles, and accumulation of autophagic material in skeletal muscle fibers.[2]

Pompe disease is typically characterized by broad clinical variability, with a phenotypic continuum that ranges from infantile-onset forms, characterized by cardiomyopathy and rapidly progressive course, to late-onset phenotypes associated with attenuated course and predominant involvement of skeletal muscles. Central nervous system involvement and motor neuron dysfunction are emerging as additional features of Pompe disease that may contribute to cognitive decline in infantile-onset forms[3] and to respiratory insufficiency.[4]

Also patients' response to enzyme replacement therapy (ERT) with recombinant human GAA (rhGAA) is highly variable. Although extraordinarily effective in some patients and on some aspects of the disease (most notably survival and cardiomyopathy in infantile patients; motor and respiratory function in late-onset forms), in other patients ERT results in minor effects in specific muscles with signs of continuing disease progression.[5]

Due to this variability, assessing patient status and response to ERT is a critical issue in the management of Pompe disease. In this respect, a major challenge is the need for reliable, measurable, and objective disease markers that are not

[1]Department of Translational Medical Sciences, Federico II University, Naples, Italy; [2]Telethon Institute of Genetics and Medicine, Pozzuoli, Italy; [3]Istituto per le Applicazioni del Calcolo Mauro Picone, Naples, Italy; [4]Department of Neurosciences, University of Messina, Messina, Italy; [5]Department of Biochemistry, Biophysics and General Pathology, Medical Genetics, University of Campania "L. Vanvitelli", Naples, Italy; [6]Department of Neurosciences, University of Torino, Torino, Italy; [7]Department of Neurosciences, Federico II University, Naples, Italy; [8]Ospedale Pediatrico Bambino Gesù, Rome, Italy; [9]Azienda Ospedaliera Universitaria Santa Maria della Misericordia, Udine, Italy; [10]Center for Lysosomal and Metabolic Diseases, Erasmus MC University Medical Center, Rotterdam, The Netherlands. Correspondence: Giancarlo Parenti parenti@unina.it, parenti@tigem.it)

Submitted 6 February 2018; accepted: 15 June 2018
Published online: 12 July 2018

influenced by inter- and intrainvestigator variance. Particularly, the degree of muscle involvement remains difficult to assess. Currently, clinical tests (muscle strength, muscle function, patient-reported outcomes) are in common use to this purpose.[6] Although several of these tests have been specifically validated for Pompe disease,[7–9] they still present some caveats. In particular, some of them appear to be specific for subsets of patients and require specific medical skills and collaboration by patients. Key factors in evaluating the reliability of tests to assess muscular involvement in Pompe disease are their clinical relevance and the minimal clinically important difference,[9] which for some of these tests needs to be further established. Biochemical or imaging-based tests include the evaluation of the glucose tetrasaccharide (GLC4)[10] in plasma and urine, muscle ultrasound,[11] muscle nuclear magnetic resonance .[12] However, the clinical relevance of the latter tests also requires further assessment.

We explored the possibility to use microRNAs (miRNAs) as disease markers in Pompe disease. miRNAs are small noncoding RNAs that regulate gene expression by targeting messenger RNAs. miRNAs are able to concurrently target multiple effectors of pathways in the context of a functional gene network, thereby finely regulating multiple cellular functions involved in disease development and progression.[13–15] In several other disease conditions, including muscular dystrophies,[16] the analysis of miRNA expression has led to the discovery of altered pathways in response to disease,[17] and has highlighted potential targets of therapeutic intervention. Because miRNAs are variably dysregulated in these disorders, their expression profile may represent a potential biomarker in diagnostic and prognostic applications.

In this study, we comprehensively analyzed by next-generation sequencing (NGS)-based procedures the expression of miRNAs in muscle and heart of a Pompe disease murine model, and in patients' plasma, with the aim to identify tools to assess patient clinical conditions and response to treatments.

MATERIALS AND METHODS

A Gaa-/- knockout Pompe disease mouse model obtained by insertion of neo into the *Gaa* gene exon 6 (ref. [18]) was purchased from Charles River Laboratories (Wilmington, MA), and was maintained at the Cardarelli Hospital's Animal Facility (Naples, Italy).

Animal studies were performed according to the EU Directive 86/609, regarding the protection of animals used for experimental purposes, and according to Institutional Animal Care and Use Committee (IACUC) guidelines for the care and use of animals in research. The study was approved by the Italian Ministry of Health, IACUC n. 523/2015-PR (06/11/2015). Every procedure on the mice was performed with the aim of ensuring that discomfort, distress, pain, and injury would be minimal. Mice were euthanized following ketamine xylazine anesthesia.

miRNAs expression profiles were analyzed by small RNA-seq in the Pompe disease mouse model (Gaa-/-)[18] in comparison with wild-type animals. We analyzed two of the main disease target tissues, i.e., heart and gastrocnemius muscle, from Pompe disease and age-matched wild-type mice. The tissues were collected at different time-points (3 and 9 months) that reflect different stages of disease progression. After small-RNA sequencing, a bioinformatic analysis was carried out to assess the reliability and statistical relevance of data (Supplementary Fig. S1). The threshold value for significance used to define up-regulation or down-regulation of miRNAs was a false discovery rate (FDR) lower than 0.05.

Plasma samples from 52 Pompe disease patients were already available and stored at −80 °C at the biobanks of the seven collaborating centers (Department of Translational Medical Sciences Federico II University, Naples; Department of Neurosciences, Federico II University, Naples; Department of Neurosciences, University of Messina; Bambino Gesù Hospital in Rome; Centre for Rare Disease, Udine; Department of Neurosciences, University of Turin; Center for Lysosomal and Metabolic Diseases; and Department of Pediatrics, Erasmus University Medical Center, Rotterdam). In all patients the diagnosis was confirmed by enzymatic analysis and *GAA* gene sequencing. Plasma had been obtained according to standard procedures during periodic follow-up admissions to the respective hospitals. Patients (or their legal guardians) had signed an informed consent agreeing that the samples would be stored and used for possible future research purposes.

Samples from age-matched controls were analyzed for comparison. Pediatric control samples derived from residual and unused amounts of plasma collected for routine chemistry in patients undergoing minor urologic surgical procedures (phimosis, hypospadias), and did not require additional medical procedures. Patients or their legal guardians consented to the use of these samples for research purposes. Juvenile and adult control samples were obtained by healthy volunteers, who consented to the use of their blood for research.

Each patient code is composed of a two-letter code identifying the city of the collaborating center, and a progressive number assigned at the time of arrival at our lab.

Total RNA extraction preserving miRNA fraction

Total RNA, including small RNAs, was extracted using the miRNeasy Kit (Qiagen) according to the manufacturer's instructions. RNA was quantified using a NanoDrop ND-8000 spectrophotometer (NanoDrop Technologies) and the integrity was evaluated using an RNA 6000 Nano chip on a Bioanalyzer (Agilent Technologies). Only samples with an RNA integrity number (RIN) >8.0 were used for library preparation.

Small RNA-seq analysis in tissues

Small RNA libraries were constructed using a Truseq small RNA sample preparation kit (Illumina) following the manufacturer's protocol. Using multiplexing, we combined

up to 12 samples into a single lane to obtain sufficient coverage. Equal volumes of the samples that constituted each library were pooled together immediately prior to gel purification and the 147–157 bp products from the pooled indexes were purified from a 6% polyacrylamide gel (Invitrogen). Libraries have been quality-checked using a DNA 1000 chip on a Bioanalyzer (Agilent Technologies) and quantified using the Qubit® 2.0 Fluorometer (Invitrogen). The sequencing was carried out by the NGS Core Facility at TIGEM, Naples. Cluster generation was performed on a Flow Cell v3 (TruSeq SR Cluster Kit v3; Illumina) using cBOT and sequencing was performed on the Illumina HiSeq1000 platform, according to the manufacturer's protocol. Each library was loaded at a concentration of 10 pM, which we had previously established as optimal.

Small RNA-seq analysis in plasma

For plasma preparation EDTA was used as anticoagulant, both in patients and in mouse samples. Processing of samples from Pompe disease and control sets were conducted simultaneously to minimize batch effect. Prior to RNA extraction, a *C. elegans*-specific synthetic exogenous miRNA (ce-miR-39) was spiked in the samples as control for the extraction efficiency. RNA was isolated using the miRNeasy Kit (Qiagen) and reverse-transcription polymerase chain reaction (RT-PCR) was performed using miScript System (Qiagen). RNA recovery was assessed by comparing the Ct values (obtained with the assay targeting the synthetic miRNA) with a standard curve of the synthetic miRNA generated independently of the RNA purification procedure. After assessment of RNA recovery, equal amounts based on starting volume (3 µl) were used for the preparation of small RNA libraries, as described for tissues. NextSeq 500/550 High Output Kit v2 (75 cycles) Cd. FC-404-2005 was used and sequencing was performed on the Illumina NextSeq 500 platform, according to the manufacturer's protocol. Each library was loaded at a concentration of 1.8 pM, previously established as optimal.

Bioinformatics analysis

To identify differentially expressed miRNAs (DE-miRNAs) across samples, the reads were trimmed to remove adapter sequences and low-quality ends, and reads mapping to contaminating sequences (e.g., ribosomal RNA, phIX control) were filtered out. The filtered reads of tissue samples were aligned to mouse mature miRNAs (miRBase Release 20), while filtered reads of plasma samples were aligned to human mature miRNAs using CASAVA software (Illumina). The comparative analysis of miRNA levels across samples was performed with edgeR,[19] a statistical package based on generalized linear models, suitable for multifactorial experiments.

Gene Ontology and KEGG pathway enrichment analysis of miRNA targets, predicted by TargetsScan,[20] was performed using the goana and kegga functions of Limma,[21] with FDR <0.05 as threshold for significant enrichment.

Quantitative real-time polymerase chain reaction (qRT-PCR) of miRNA

Expression of mature miRNAs was assayed using Taqman Advanced MicroRNA Assay (Applied Biosystems) specific for miRNA selected for validation. qRT-PCR was performed by using an Applied Biosystems 7900 Fast-Real-time PCR System and a TaqMan Fast Advanced Master Mix. Primers for selected miRNAs were obtained from the TaqMan Advanced miRNA Assays. Samples were run in duplicate. Single TaqMan microRNA assays were performed according to manufacturer's instructions (Applied Biosystems). Differences in miRNAs expression, expressed as fold changes, were calculated using the 2-ΔΔCt method. In plasma samples, to calculate ΔCts values, the average of two normalizers was used: spike in ce-miR-39 and endogenous stable miRNA miR-93 (ref. [22]). Next, to calculate ΔΔCt values an average of five controls, each of them analyzed in three independent experiments, was used. miR-16 was used as endogenous normalizer in tissue samples.

In vivo experiments in the Pompe disease mouse model

Pompe disease mice received a single high-dose (100 mg/kg) injection of Myozyme into the retroorbital vein. Tissues (heart, gastrocnemius) were collected 48 h after the injection and miR-133 was analyzed by qRT-PCR as indicated.

The results obtained were compared with those obtained in control animals injected with equivalent volumes of saline. Four animals for each group were analyzed.

Statistical analysis

Group-wise comparisons (Fig. 4**a**) were performed by two-way analysis of variance (ANOVA) with Tukey post hoc test. A Student's *t* test was used for the statistical analysis of the data shown in Fig. 4**d** and Supplementary Fig. S2.

RESULTS

Global analysis of miRNA expression profiles in the skeletal muscle and heart of the Pompe disease mouse model

The small RNA-seq analysis in tissues from the Pompe disease mouse model generated a list of 277 miRNAs that were differentially expressed (DE-miRNA) in the two tissues examined (gastrocnemius and heart) with statistical significance, compared with control mice. The complete list and the results of the sequencing are provided in Supplementary Table S1. Figure 1 provides a summary of the results obtained in the two tissues examined and at the different time-points. The patterns of miRNA dysregulation varied depending on age, indicating changes related to disease progression, and tissues, suggesting tissue-specific involvement of different pathways. The DE-miRNA were either up-regulated or down-regulated.

Pompe disease patients show differential expression of circulating miRNAs

We then looked at plasma samples from patients affected by Pompe disease. We decided to perform a small RNA-seq

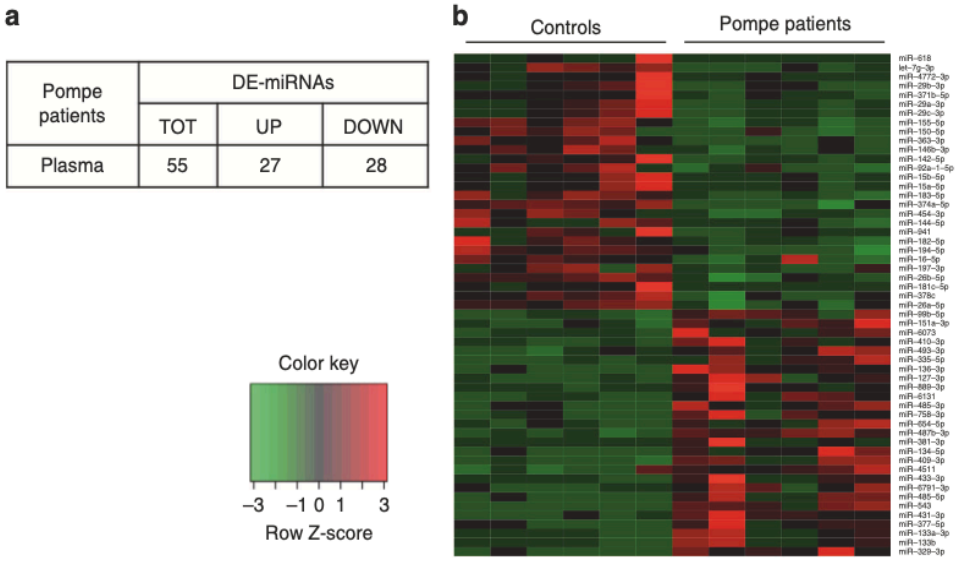

Fig. 2 Results of small-RNA-seq analysis in Pompe disease patient plasma. (**a**) Summary of the number of differentially expressed microRNA (DE-miRNA) up- and down-regulated. (**b**) Heatmap of the 55 DE-miRNAs up-regulated (red) or down-regulated (green)

Table 1 miRNAs dysregulated both in Pompe mice tissues and in patient plasma

DE-miRNAs	Pompe patients	Pompe KO mouse	
	Plasma	Gastrocnemius	Heart
miR-127-3p	↑	↓	
miR-136-3p	↑	↓	
miR-182-5p	↓	↑	
miR-133a-3p	↑	↓	
miR-142-5p	↓	↑	↑
miR-155-5p	↓	↑	
miR-15b-5p	↓	↑	↑
miR-26a-5p	↓	↓	
miR-26b-5p	↓	↓	
miR-29c-3p	↓	↓	↓
miR-410-3p	↓	↓	
miR-144-5p	↓	↓	↓
miR-183-5p	↓	↑	
miR-329-3p	↑	↓	
miR-92a-1-5p	↓	↑	
miR-99b-5p	↑	↑	

The arrow's direction indicates the up- or down-regulation
DE-miRNA differentially expressed microRNA, *KO* knockout

were compared with control samples obtained from age-matched pediatric patients, while the results obtained in LOPD were compared with those of age-matched healthy volunteers.

We found 55 miRNAs that were differentially expressed with an FDR <0.05 (the complete list is provided in Supplementary Table 3) and that were either up- or down-regulated (Fig. 2). Sixteen miRNAs were differentially expressed both in tissues from Pompe disease mice and in patient plasma (Table 1). For the majority of these miRNAs the pattern of expression was different in the two species. However, this was not surprising, considering the different sources of biological samples and patient clinical heterogeneity.

The DE-miRNAs in Pompe disease are involved in pathways that are potentially relevant for the disease pathophysiology

A literature analysis indicates that the 16 DE-miRNAs that are dysregulated both in mouse tissues and in patients' plasma have been linked, as expected, to multiple function and pathways. The majority of them are reported to be involved in cancer-related processes, likely due to the preponderant number of studies in the literature that are focused on the role of miRNAs in cancer.

Interestingly, some DE-miRNAs are involved in pathways that are of potential relevance for Pompe disease pathophysiology, such as muscle cell proliferation, regeneration and differentiation (miR-127, miR-133, miR-136, miR-142, miR-329), autophagy (miR-26, miR-29c, miR-142, miR-183), apoptosis (miR15b, miR-26, miR-29c, miR-136, miR-144, miR-410), endoplasmic reticulum/oxidative stress (miR15b, miR-99, miR-133, miR-155, miR-144, miR-329), muscle metabolism and insulin response (miR-26, miR-29c, miR-182), inflammation (miR-142, miR-155, miR-410), fibrosis (miR-29c, miR-410), cardiomyopathies (miR-26, miR-133, miR-182, miR-410), and atrophy (miR-182). The finding of dysregulation of miRNAs involved in the process of atrophy may also be compatible both with primary muscle atrophy and with denervation atrophy.

To gather more information on the processes in which the DE-miRNAs can be functionally involved, we carried out Gene Ontology and KEGG pathway enrichment analysis using as queries the list of their predicted targets identified through TargetScan.[20] The most recurrent target genes in the most frequently enriched KEGG pathways (genes that are predicted target of at least four DE-miRNAs) are shown in Fig. 3.

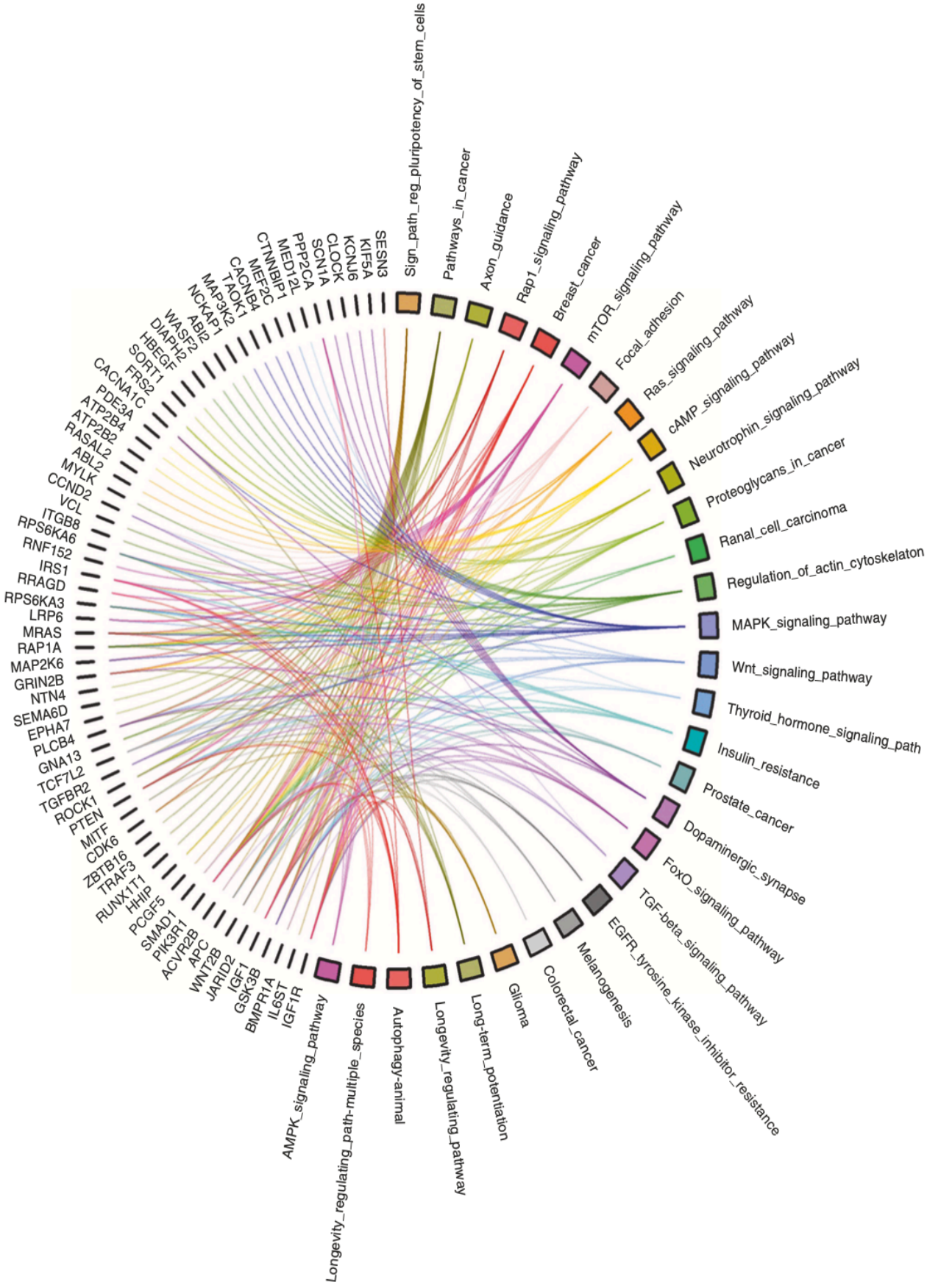

Fig. 3 Bioinformatic analysis of differentially expressed microRNA (DE-miRNA) targets. Circos plots of the most frequent pathways (right from top to bottom) and most frequent genes (left from bottom to top) predicted to be targeted by the 16 common DE-miRNAs

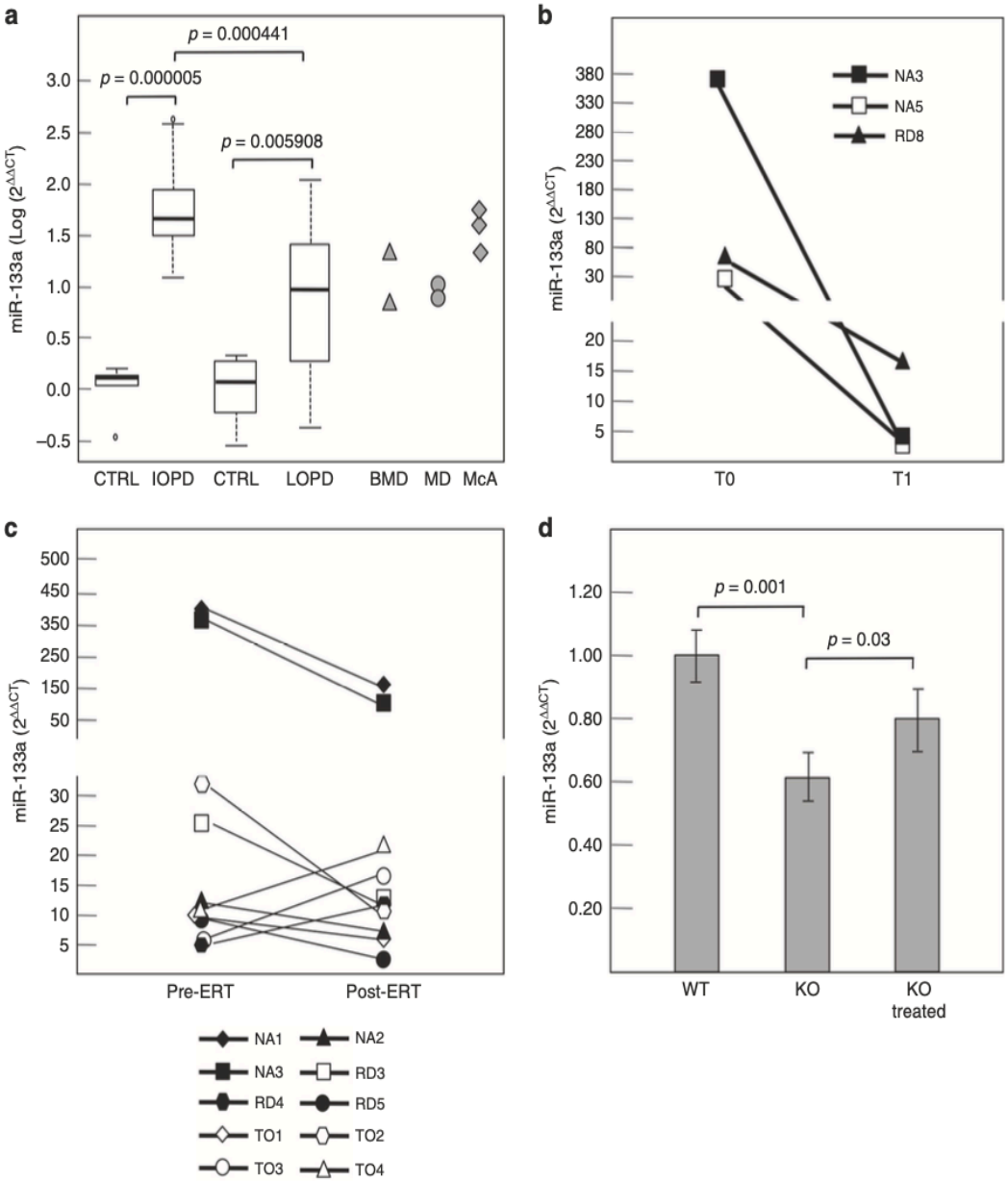

Fig. 4 Expression level of circulating miR-133a and effect of therapy. a In infantile-onset Pompe disease (IOPD) patients miR-133a levels were significantly ($p = 0.000005$) higher (12.44- to 414.96-fold) than those of age-matched controls. IOPD patients had significantly higher levels compared with late-onset Pompe disease (LOPD) patients ($p = 0.000441$). In LOPD patients miR-133a was also significantly increased ($p = 0.005908$) compared with age-matched controls. *P* analysis of variance (ANOVA) = 0.03662. miR-133a was also elevated in patients with other myopathies, including Becker muscular dystrophy (BMD, gray triangles), Steinert myotonic dystrophy (MD, gray circles), McArdle muscle (McA, gray diamonds). **b** Expression level of miR-133a in plasma from 3 IOPD. For each patient, miR-133a was analyzed before first enzyme replacement therapy (ERT) infusion (T0) and after 3 years of treatment (NA3), 7 months (NA5), and 3 years and 3 months (RD8) (T1), and after near-complete correction of clinical manifestations. **c** Expression level of miR-133a in plasma from 10 PD patients pre-ERT infusion and 24 h post-ERT. **d** Effect of a single high-dose infusion of rhGAA (100 mg/kg). Expression of miR-133a was analyzed in gastrocnemii from 9-month-old Pompe disease mice, compared with wild-type age-matched animals and 48 h after rhGAA infusion. KO knockout, WT wild-type

As a result, we found that a number of DE-miRNAs and their target genes are involved in processes that are potentially relevant for Pompe disease pathophysiology (Fig. 3), like MAPK, FoxO, mTOR, AMPK and insulin signaling pathways, ubiquitin-mediated proteolysis, cardiac hypertrophy, fibrosis, muscle atrophy and regeneration, autophagy, regulation of stem cells pluripotency, and myogenesis. We also found some DE-miRNAs that are implicated in other pathways, such as oxidative stress and inflammation, that have occasionally been associated with Pompe disease.[23, 24] Some DE-miRNAs are involved in more than one of these pathways, which suggests that they play a significant role in Pompe disease pathophysiology, and in an intricate interplay between secondary cellular events triggered in response to glycogen storage.

miR-133a levels correlate with Pompe disease clinical forms

We selected one of the miRNAs, miR-133a, that were differentially expressed both in Pompe disease mice and in

patients for further validation and confirmation by qRT-PCR. The analysis was performed in patients' plasma from all 52 patients. Information on these patients is provided in Supplementary Table S2. Ten of the patients were affected by IOPD, whereas 42 had LOPD.

miR-133a has been reported to be a member of the myogenic miRNAs (so-called Myo-miRs);[25] is expressed in the skeletal and cardiac muscles of mammals, birds and zebrafish; and is dysregulated in cardiac hypertrophy and other cardiac disorders,[26] and in muscular dystrophies.[16, 27]

qRT-PCR analysis showed minor variations of miR-133a levels with respect to age in controls (Fig. 4a), with slightly higher levels in younger individuals. Conversely, quantitative analysis confirmed that miR-133a is up-regulated in Pompe disease patients (Fig. 4a), as already observed by small RNA-seq. In IOPD patients miR-133a levels were significantly ($p = 0.000005$) higher (12.44 to 414.96-fold) than those of age-matched controls and did not overlap with controls. IOPD patients had the highest levels of miR-133a, which were significantly higher than those observed in LOPD patients ($p = 0.000441$). In LOPD patients miR-133a was also significantly increased ($p = 0.005908$) compared with age-matched controls, but with lower levels, with a broader distribution of values, and with some overlap between controls and LOPD patients.

As positive control, we performed the analysis in samples from two patients affected by Becker muscular dystrophy. In addition, we analyzed samples from patients with other myopathies, including three patients with McArdle glycogenosis and two patients with Steinert myotonic dystrophy. Compared with age-matched controls all these patients showed increased miR-133a levels (Fig. 4a).

We also measured miR-133a levels in plasma from the murine Pompe disease model. MiR-133a was modestly elevated only in older mice (15 months of age) (Supplementary Fig. S2). Considering that the phenotype observed in the knockout mouse is relatively mild (with the exception of the presence of cardiomyopathy) and allows for near normal survival and fertility, these data are not surprising.

ERT affects circulating miR-133a levels in Pompe disease

We then tested whether miR-133a levels are influenced by ERT with rhGAA. Only for 3 IOPD patients (NA3, NA5, RD8) were stored plasma samples available, which had been obtained before starting ERT (T0), at the age of 9, 2 and 3 months respectively. Before starting ERT all patients showed the full clinical picture of IOPD, with hypertrophic cardiomyopathy and severe hypotonia. In the pre-ERT samples miR-133a levels were high. After 3 years of treatment (NA3), 7 months (NA5), and 3 years and 3 months (RD8), respectively, a good clinical response to ERT had already been achieved in all patients, with near-complete correction of cardiac hypertrophy as assessed by cardiac ultrasound scan, and adequate motor function for age. At that time plasma miR-133a levels were substantially decreased in all patients (Fig. 4b), suggesting a correlation between miRNA levels and the effects of treatment.

We also analyzed the effects of single ERT infusions in ten patients, for which samples before and 24 h after an ERT infusion were available in our laboratories (Fig. 4c). One of these samples (NA3) had been obtained after the first ERT infusion and pretreatment levels corresponded to those shown in Fig. 4b. All other patients had already been treated for variable periods. All patients displayed up-regulation of miR-133a before ERT with respect to the mean of control samples. In seven patients the level of miR-133a decreased after ERT, with most evident decreases in the patients with the highest miR-133a preinfusion levels.

We also tested the effect of a single infusion of rhGAA in the Pompe disease mouse model. As previously shown, in the Pompe mouse miR-133a is down-regulated in gastrocnemius, while in heart it is normally expressed. We gave a single injection of rhGAA at a high dose (100 mg/kg) to obtain detectable changes in miR-133a expression. Forty-eight hours after the injection, tissues were collected and analyzed by qRT-PCR. In gastrocnemius miR-133a levels returned to values that are close to those measured in wild-type animals (Fig. 4d), while no changes were observed in heart (not shown).

DISCUSSION

In this study we have evaluated whether miRNA profiles may represent potential biomarkers for Pompe disease. Small RNA-seq was selected as a tool to analyze miRNA expression because this approach is well suited for large-scale quantitative analysis of nucleotide sequences.

The design of the study, with an initial step in which we first performed the small RNA-seq analysis in the Pompe disease mouse model and subsequently in a selected number of patients, represented a compromise between the potential of NGS and the costs of this methodology. An advantage of using the animal model was the possibility to run our preliminary analysis in a homogenous sample, with a common genetic background and uniform disease progression, and to look at the tissues that are most affected by disease pathology. This initial approach allowed us to identify and select a restricted number of miRNAs that are dysregulated in Pompe disease. These miRNAs were subjected to a bioinformatic analysis to gather information on their possible role in Pompe disease pathophysiology.

The DE-miRNAs that we selected in this way were (1) dysregulated in Pompe disease (both in mice tissues and in patients' plasma); (2) potentially relevant for the disease pathophysiology according to the bioinformatic and literature analysis; and (3) measurable in samples, like plasma, that are readily available in Pompe disease patients and in general require minimally invasive procedures.

One of these miRNAs was further validated in the whole cohort of our patients by qRT-PCR. miR-133a was particularly attractive, because it had already been proposed as a biomarker for Duchenne/Becker muscular dystrophy,[16] and

because it has been shown to be involved in processes including muscle regeneration, atrophy, and inflammation.

Both in IOPD and in LOPD patients miR-133a was significantly elevated. However, the levels observed in IOPD were significantly higher compared with those measured in patients with attenuated phenotypes, suggesting a correlation between miR-133a levels and the clinical forms of the disease. This difference was not due to an age-related effect, because in age-matched controls miR-133a levels were only modestly higher than those obtained at later ages.

While in IOPD patients, who show a more homogeneous phenotype,[28–30] we consistently found increased miR-133a levels, the results in LOPD showed marked variability. It was thus impossible, in a relatively limited number of patients, to establish clear correlations between individual parameters (such as age, diseases stage, clinical scores, motor performance, need for ventilator support). It is reasonable to think that in LOPD patients, who show an extremely broad rage of phenotypes,[31] several factors (muscle mass, fibrosis, in addition to age, disease severity, etc.) concomitantly contribute to the expression of miR-133a and to its plasma levels. We believe that studies in larger cohorts of patients, based on the concerted effort of international consortia and on the collaboration of the leading centers in the follow-up of Pompe disease patients, may further validate the results of our study, and address possible correlations between miRNA levels and LOPD patient status, response to therapy, or outcome.

An important finding of our study is that miR-133a levels showed a trend toward decrease in response to ERT. Samples before the start of treatment were only available for three patients. In all of them we found a clear decrease of miR-133a, concomitant to overt clinical improvement. miR-133a levels also decreased in seven of ten patients even after a single injection after ERT treatment. In addition, we found normalization of miR-133a in gastrocnemii from Pompe disease animals after single injection of high-dose rhGAA. Our results suggest that miR-133a may represent an adjunct marker of ERT effects, to be used in combination with clinical and biochemical measures.

The availability of a broad range of reliable tests appears particularly important for the development of guidelines for patient monitoring, for ERT inclusion and exclusion criteria that are currently being defined in some countries,[32] to correlate different ERT regimens and patient response to treatment, and to optimize and personalize treatment protocols. In addition, disease markers that provide information on Pompe disease pathophysiology may allow for identification of dysregulated pathways, new therapeutic targets, and, possibly, for development of novel therapeutic strategies.

We chose to use one DE-miRNA as a measurable marker in our cohort of Pompe disease patients. However, should the costs of NGS become more affordable (as is indeed expected in the coming years, thanks to the development of second-generation technologies and more flexible instruments), this approach may be proposed to collect a large body of data that may be even more informative in patient follow-up and allow for the identification of a specific "signature" of Pompe disease, and of disease progression, outcome, or response to therapies.

ELECTRONIC SUPPLEMENTARY MATERIAL

The online version of this article (https://doi.org/10.1038/s41436-018-0103-8) contains supplementary material, which is available to authorized users.

ACKNOWLEDGEMENTS

This study would have never been possible without the support of the Acid Maltase Deficiency Association (AMDA, Helen Walker Research Grant, 2014 to GP). This work was supported in part by the Italian Agency of Medicines (AIFA-2016-02364305 grant to GP). We thank the TIGEM NGS and Bioinformatic cores for their work, Roberta Tarallo, Laura Marra, Giovanni Nassa, and Giorgio Giurato for helpful suggestions. We thank Graciana Diez-Roux for manuscript revision.

DISCLOSURE

The authors declare that they have no conflicts of interest.

REFERENCES

1. van der Ploeg AT, Reuser AJ. Pompe's disease. *Lancet*. 2008;372:1342–1353.
2. Shea L, Raben N. Autophagy in skeletal muscle: implications for Pompe disease. *Int J Clin Pharmacol Ther*. 2009;47(suppl 1):S42–47.
3. Ebbink BJ, Poelman E, Classic infantile Pompe patients approaching adulthood: a cohort study on consequences for the brain. *Dev Med Child Neurol*. 2018;60:579–586.
4. Fuller DD, ElMallah MK. The respiratory neuromuscular system in Pompe disease. *Respir Physiol Neurobiol*. 2013;189:241–249.
5. Prater SN, Banugaria SG, DeArmey SM, et al. The emerging phenotype of long-term survivors with infantile Pompe disease. *Genet Med*. 2012;14:800–810.
6. Schoser B, Laforet P, Kruijshaar ME, et al. 208th ENMC International Workshop: formation of a European Network to develop a European data sharing model and treatment guidelines for Pompe disease Naarden, The Netherlands, 26-28 September 2014. *Neuromuscul Disord*. 2015;25:674–678.
7. Angelini C, Semplicini C, Ravaglia S, et al. New motor outcome function measures in evaluation of late-onset Pompe disease before and after enzyme replacement therapy. *Muscle Nerve*. 2012;45:831–834.
8. van der Beek NA, Hagemans ML, van der Ploeg AT, van Doorn PA, Merkies IS. The Rasch-built Pompe-specific activity (R-PAct) scale. *Neuromuscul Disord*. 2013;23:256–264.
9. Lachmann R, Schoser B. The clinical relevance of outcomes used in late-onset Pompe disease: can we do better? *Orphanet J Rare Dis*. 2013;8:160.
10. Young SP, Zhang H, Corzo D, et al. Long-term monitoring of patients with infantile-onset Pompe disease on enzyme replacement therapy using a urinary glucose tetrasaccharide biomarker. *Genet Med*. 2009;11:536–541.
11. Vill K, Schessl J, Teusch V, et al. Muscle ultrasound in classic infantile and adult Pompe disease: a useful screening tool in adults but not in infants. *Neuromuscul Disord*. 2015;25:120–126.
12. Pichiecchio A, Uggetti C, Ravaglia S, et al. Muscle MRI in adult-onset acid maltase deficiency. *Neuromuscul Disord*. 2004;14:51–55.
13. Bushati N, Cohen SM. microRNA functions. *Annu Rev Cell Dev Biol*. 2007;23:175–205.
14. Bartel DP. MicroRNAs: target recognition and regulatory functions. *Cell*. 2009;136:215–233.
15. Pasquinelli AE. MicroRNAs and their targets: recognition, regulation and an emerging reciprocal relationship. *Nat Rev Genet*. 2012;13:271–282.

16. Cacchiarelli D, Legnini I, Martone J, et al. miRNAs as serum biomarkers for Duchenne muscular dystrophy. *EMBO Mol Med*. 2011;3:258–265.
17. Allegra A, Alonci A, Campo S, et al. Circulating microRNAs: new biomarkers in diagnosis, prognosis and treatment of cancer (review). *Int J Oncol.* 2012;41:1897–1912.
18. Raben N, Nagaraju K, Lee E, et al. Targeted disruption of the acid alpha-glucosidase gene in mice causes an illness with critical features of both infantile and adult human glycogen storage disease type II. *J Biol Chem*. 1998;273:19086–19092.
19. Robinson MD, McCarthy DJ, Smyth GK. edgeR: a Bioconductor package for differential expression analysis of digital gene expression data. *Bioinformatics*. 2010;26:139–140.
20. Chiang HR, Schoenfeld LW, Ruby JG, et al. Mammalian microRNAs: experimental evaluation of novel and previously annotated genes. *Genes Dev*. 2010;24:992–1009.
21. Ritchie ME, Phipson B, Wu D, et al. limma powers differential expression analyses for RNA-sequencing and microarray studies. *Nucleic Acids Res*. 2015;43:e47.
22. Perfetti A, Greco S, Cardani R, et al. Validation of plasma microRNAs as biomarkers for myotonic dystrophy type 1. *Sci Rep*. 2016;6:38174.
23. Palermo AT, Palmer RE, So KS, et al. Transcriptional response to GAA deficiency (Pompe disease) in infantile-onset patients. *Mol Genet Metab*. 2012;106:287–300.
24. Lim JA, Li L, Shirihai OS, Trudeau KM, Puertollano R, Raben N. Modulation of mTOR signaling as a strategy for the treatment of Pompe disease. *EMBO Mol Med*. 2017;9:353–370.
25. Lagos-Quintana M, Rauhut R, Meyer J, Borkhardt A, Tuschl T. New microRNAs from mouse and human. *RNA*. 2003;9:175–179.
26. Liu Y, Liang Y, Zhang JF, Fu WM. MicroRNA-133 mediates cardiac diseases: mechanisms and clinical implications. *Exp Cell Res*. 2017;354:65–70.
27. Zaharieva IT, Calissano M, Scoto M, et al. Dystromirs as serum biomarkers for monitoring the disease severity in Duchenne muscular dystrophy. *PLoS ONE*. 2013;8:e80263.
28. van den Hout HM, Hop W, van Diggelen OP, et al. The natural course of infantile Pompe's disease: 20 original cases compared with 133 cases from the literature. *Pediatrics*. 2003;112:332–340.
29. Kishnani PS, Corzo D, Nicolino M, et al. Recombinant human acid [alpha]-glucosidase: major clinical benefits in infantile-onset Pompe disease. *Neurology*. 2007;68:99–109.
30. Kishnani PS, Hwu WL, Mandel H, et al. A retrospective, multinational, multicenter study on the natural history of infantile-onset Pompe disease. *J Pediatr*. 2006;148:671–676.
31. Kroos M, Hoogeveen-Westerveld M, Michelakakis H, et al. Update of the Pompe disease mutation database with 60 novel GAA sequence variants and additional studies on the functional effect of 34 previously reported variants. *Hum Mutat*. 2012;33:1161–1165.
32. van der Ploeg AT, Kruijshaar ME, Toscano A, et al. European consensus for starting and stopping enzyme replacement therapy in adult patients with Pompe disease: a 10-year experience. *Eur J Neurol*. 2017;24:768–e731.

General Conclusion

While the biochemistry and genetics of PD are well known already for many years, its pathophysiology is still incompletely understood. Through electron microscopy it has been possible to observe how muscle cells affected by PD show an abnormal accumulation of autophagosomes, probably connected to a malfunction of the autophagic process. This would not only damage the muscle fibers, destroying their normal architecture, but would also prevent the correct targeting of the exogenous enzyme within the cells, which would not be able to reach the destination site, the lysosome, remaining trapped in the autophagic area. The characterization of these pathways is particularly important since secondary abnormalities may represent novel targets of therapy. Also, identifying new reliable biomarkers to monitor of disease progression and of efficacy of therapies, is still a major need in the management of patients'.

The scope of the present work was to address these issues. We have investigated:

a) The status of oxidative-stress and autophagic pathways in PD and the effects of their pharmacological manipulation as an adjunctive therapy for PD patients'

b) miRNAs as biomarkers in PD

a) Characterization of the oxidative-stress and autophagic pathways in PD.

The derangement of secondary pathways is emerging as an important factor in many LSDs, including PD. A detailed characterization of the autophagic and oxidative-stress pathways has important implications. On one hand these studies will provide new information on the disease pathophysiology, on the other hand they are potentially relevant for the identification of novel therapeutic targets. Thus, after characterizing the status of these pathways, I explored the possibility to manipulate them pharmacologically and to find new therapeutic strategies. I have provided several lines

of evidence supporting the presence of increased oxidative-stress in PD, both in vitro (fibroblasts from patients) and in vivo, in the PD mouse model. I also showed that oxidative-stress is related to the impairment of the autophagic pathway. The ultimate goal of my studies was to improve the efficacy of ERT, in order to address some of the limitations of this approach. This may translate into improved outcome and quality of life for patients. Since the compounds that we have tested as therapeutic agents are in most cases already approved for clinical use, a possible translation of our results into clinical studies could be immediate.

b) **miRNAs as biomarkers in PD**

Insufficient delivery of the therapeutic enzyme to target tissues, with incomplete correction of pathology in skeletal muscles, has been extensively documented in PD animal models and in patients. The aim of this part of my project was to identify new reliable biomarkers to monitor of disease progression and of efficacy of therapies. We explored the possibility to use microRNAs (miRNAs) as disease markers in PD. In our work we found:

- 198 miRNAs differentially expressed with statistical significance in gastrocnemius and 66 DE-miRNAs in heart in mouse model
- 55 miRNAs differentially expressed in patients' plasma.

One of these microRNAs, miR-133a, was selected for further quantitative real-time polymerase chain reaction analysis in plasma samples from 52 patients, obtained from seven Italian and Dutch biobanks. miR-133a levels were significantly higher in PD patients than in controls and correlated with phenotype severity, with higher levels in infantile compared with late-onset patients. In three infantile patients miR-133a decreased after start of enzyme replacement therapy and evidence of clinical improvement. Expanding the cohort of patients and identifying more miRNAs will allow

us to establish possible relationships between miRNAs and ERT or disease progression.

Bibliography

Angelini C, Semplicini C, Ravaglia S, Moggio M, Comi GP, Musumeci O, Pegoraro E, Tonin P, Filosto M, Servidei S, Morandi L, Crescimanno G, Marrosu G, Siciliano G, Mongini T, Toscano A; Italian Group on GSDII. New motor outcome function measures in evaluation of late-onset Pompe disease before and after enzyme replacement therapy. Muscle Nerve. 2012. Jun;45(6):831-4.

Babior BM. Phagocytes and oxidative stress. The American Journal of Medicine. 2000;109:33–44.

Bodamer OA, Scott CR, Giugliani R; Pompe Disease Newborn Screening Working Group. Newborn Screening for Pompe Disease. Pediatrics. 2017;140(Suppl 1):S4-S13.

Chien Y, Hwu W, Lee N. Newborn screening: Taiwanese experience. Ann Transl Med. 2019;7(13):281.

Chuang YY, Chen Y, Gadisetti, Chandramouli VR, Cook JA, Coffin D, Tsai MH, DeGraff W, Yan H, Zhao S, Russo A, Liu ET, Mitchell JB. Gene expression after treatment with hydrogen peroxide, menadione, or t-butyl hydroperoxide in breast cancer cells. Cancer Research. 2002; 62:6246–54.

Cuervo A.M. Chaperone-mediated autophagy: Selectivity pays off. Trends Endocrinol. Metab. 2010;2142–150.

Filomeni G, De Zio D and Cecconi F. Oxidative stress and autophagy: the clash between damage and metabolic needs. Cell Death Differ. 2015; 22(3): 377–388.

Fukuda T, Ahearn M, Roberts A, Mattaliano RJ, Zaal K, Ralston E, Plotz PH, Raben N. Autophagy and Mistargeting of Therapeutic Enzyme in Skeletal Muscle in Pompe disease. Mol Ther. 2006; 14:831-9.

Hagemans ML, Winkel LP, Van Doorn PA, Hop WJ, Loonen MC, Reuser AJ, Van der Ploeg AT. Clinical manifestation and natural course of late-onset Pompe's disease in 54 Dutch patients. Brain. 2005;128, 671-677.

Hirschhorn R, Reuser AJJ: Glycogen storage disease type II: acid a-glucosidase (acid maltase) deficiency. In The Metabolic and Molecular Bases of Inherited Disease 8th edition. Edited by: Scriver CR, Beaudet AL, Valle D, Sly WS. New York: McGraw-Hill, Inc. 2001; 3389-3420.

Hoefsloot LH, Hoogeveen-Westerveld M, Reuser AJ, Oostra BA. Characterization of the human lysosomal alpha-glucosidase gene. Biochem J. 1990;272: 493-497.

Hoefsloot LH, Willemsen R, Kroos MA, Hoogeveen-Westerveld M, Hermans MM, Van der Ploeg AT, Oostra BA, Reuser AJ. Expression and routeing of human lysosomal alpha-glucosidase in transiently transfected mammalian cells. Biochem J. 1990;272, 485-492.

Kara A, Gedikli S, Sengul E, Gelen V. Oxidative Stress and Autophagy. Free Radicals and Diseases. 2016.

Kim J, Kundu M, Viollet B, and Guan KL. AMPK and mTOR regulate autophagy through direct phosphorylation of Ulk1. Nat. Cell Biol. 2011;13, 132–141.

Kishnani PS, Hwu WL, Mandel H, Nicolino M, Yong F, Corzo D; Infantile-Onset Pompe Disease Natural History Study Group. A retrospective, multinational, multicenter study on the natural history of infantile-onset Pompe disease. J Pediatr. 2006;148(5), 671-676.

Kohler L, Puertollano R, Raben N. Pompe Disease: From Basic Science to Therapy. Neurotherapeutics. 2018; 15:928-42.

Lee IH, Cao L, Mostoslavsky R, Lombard DB, Liu J, Bruns NE, Tsokos M, Alt FW, and Finkel T. A role for the NAD-dependent deacetylase Sirt1 in the regulation of autophagy. Proc Natl Acad Sci USA.2008;105: 3374-3379.

Levine B. Eating oneself and uninvited guests: autophagy-related pathways in cellular defense. Cell. 2005;1 20:159–62.

Lieberman AP, Puertollano R, Raben N, Slaugenhaupt S, Walkley SU, Ballabio A. Autophagy in lysosomal storage disorders. Autophagy. 2012;8(5):719–730.

Lim J, Li L, Kakhlon O, Myerowitz R and Raben N. Defects in calcium homeostasis and mitochondria can be reversed in Pompe disease. Autophagy.2015; 11(2): 385–402.

Medina DL, Ballabio A. Lysosomal calcium regulates autophagy. Autophagy.2015; 11, 970–971.

Mizushima N, Yoshimori T, Ohsum Y. The role of Atg proteins in autophagosome formation. Annu Rev. Cell Dev Biol. 2011; 27, 107–132.

Navarro-Yepes J, Burns M, Anandhan A, Khalimonchuk O, del Razo LM, Quintanilla-Vega B, Pappa A, Panayiotidis MI, Franco R. Oxidative stress, redox signaling, and autophagy: cell death versus survival. Antioxid Redox Signal.2014;21(1): p. 66-85.

Nazio F, Cecconi F. mTOR AMBRA1, and autophagy: an intricate relationship. Cell Cycle. 2013;12:2524–2525.

Nishino I. Autophagic vacuolar myopathies. Curr Neurol Neurosci Rep. 2003;3(1):64–9.

Prater SN, Banugaria SG, DeArmey SM, Botha EG, Stege EM, Case LE, Jones HN, Phornphutkul C, Wang RY, Young SP, Kishnani PS.The emerging phenotype of long-term survivors with infantile Pompe disease. Genet Med. 2012;14:800-10.

Raben N, Danon M, Gilbert AL, Dwivedi S, Collins B, Thurberg BL, Mattaliano RJ, Nagaraju K, Plotz PH. Enzyme replacement therapy in the mouse model of Pompe disease. Mol Genet Metab. 2003;80(1-2), 159-169.

Raben N, Ralston E, Chien YH, Baum R, Schreiner C, Hwu WL, Zaal KJ, Plotz P. Differences in the predominance of lysosomal and autophagic pathologies between infants and adults with Pompe disease: implications for therapy. Mol Genet Metab. 2010; 108:1383–1388.

Ravikumar B, Sarkar S, Davies JE, Futter M, Garcia-Arencibia M, Green-Thompson ZW, Jimenez-Sanchez M, Korolchuk VI, Lichtenberg M, Luo S. Regulation of mammalian autophagy in physiology and pathophysiology. Physiol. Rev. 2010;90, 1383–1435.

Reuser AJ, Kroos MA, Ponne NJ, Wolterman RA, Loonen MC, Busch HF, Visser WJ, Bolhuis PA. Uptake and stability of human and bovine acid alpha-glucosidase in cultured fibroblasts and skeletal muscle cells from glycogenosis type II patients. Exp Cell Res.1984;155(1): p. 178-89.

Sardiello, M.; Palmieri, M.; di Ronza, A.; Medina, D.L.; Valenza, M.; Gennarino, V.A.; Di Malta, C.; Donaudy, F.; Embrione, V.; Polishchuk, R.S. A gene network regulating lysosomal biogenesis and function. Science.2009; 325, 473–477.

Scott CR, Elliott S, Buroker N, Thomas LI, Keutzer J, Glass M, Gelb MH, Turecek F. Identification of infants at risk for developing Fabry, Pompe, or mucopolysaccharidosis-I from newborn blood spots by tandem mass spectrometry. J Pediatr. 2013; 163(2):498-503.

Semplicini C, Letard P, De Antonio M, Taouagh N, Perniconi B, Bouhour F, Echaniz-Laguna A, Orlikowski D, Sacconi S, Salort-Campana E, Solé G, Zagnoli F, Hamroun D, Froissart R, Caillaud C, Laforêt; French Pompe Study Group. Late-onset Pompe disease in France: molecular features and epidemiology from a nationwide study. J Inherit Metab Dis. 2018;41(6):937-946.

Settembre C, Zoncu R, Medina DL, Vetrini F, Erdin S, Erdin S, Huynh T, Ferron M, Karsenty G, Vellard MC, Facchinetti V, Sabatini DM, Ballabio A. A lysosome-to-nucleus signalling mechanism senses and regulates the lysosome via MTOR and TFEB: self-regulation of the lysosome via MTOR and TFEB. EMBO J. 2012; 31, 1095–1108.

Shea L, Raben N. Autophagy in skeletal muscle: implications for Pompe disease. Int J Clin Pharmacol Ther. 2009; 47 Suppl 1: S42–47.

Schoser BG, Muller-Hocker J, Horvath R, et al. Adult-onset glycogen storage disease type 2: clinico-pathological phenotype revisited. Neuropathol Appl Neurobiol. 2007;33(5):544–559.

Van den Hout HM, Hop W, van Diggelen OP, Smeitink JA, Smit GP, Poll-The BT, Bakker HD, Loonen MC, de Klerk JB, Reuser AJ, van der Ploeg AT. The natural course of infantile Pompe's disease: 20 original cases compared with 133 cases from the literature. Pediatrics. 2003;112(2), 332-340.

Van den Hout H, Reuser AJ, Vulto AG, Loonen MC, Cromme-Dijkhuis A, Van der Ploeg AT. Recombinant human alpha-glucosidase from rabbit milk in Pompe patients. 2000;356(9227):397-8.

Van der Ploeg AT., Kroos M A, Willemsen R, Brons N H, and Reuser AJ. Intravenous administration of phosphorylated acid alpha-glucosidase leads to uptake of enzyme in heart and skeletal muscle of mice. J Clin Invest. 1991;87(2): p. 513-8.

Van der Ploeg AT, Reuser AJ. Pompe's disease. Lancet. 2008;372: 1342–1353.

Volpert G, Ben-Dor S, Tarcic O, Duan J, Saada A, H. Merrill A, Jr, Pewzner-Jung Y and Futerman AH. Oxidative stress elicited by modifying the ceramide acyl chain length reduces the rate of clathrin-mediated endocytosis. The Company of Biologists. 2017; 130, 1486-1493.

Wenk J, Hille A and von Figura K. Quantitation of Mr 46000 and Mr 300000 mannose 6-phosphate receptors in human cells and tissues. Biochem Int.1991; 23: 723–731.

Yang Z, Klionsky DJ. Mammalian autophagy: core molecular machinery and signaling regulation. Curr Opin Cell Biol. 2010;22:124–131.

Youle RJ and Narendra DP. Mechanisms of mitophagy.Cell Biol. 2011; 12, 9–14.

Zhang X, Cheng X, Yu L, Yang J, Calvo R, Patnaik S, Hu X, Gao Q, Yang M, Lawas M, Delling M, Marugan J, Ferrer M, Xu H. MCOLN1 is a ROS sensor in lysosomes that regulates autophagy. Nat. Commun. 2016; 7, 12109.